OPTIMIZING TEMPERATURE PARAMETERS FOR ENHANCED MINERALIZATION PROCESS: MAXIMIZING CO$_2$ CONVERSION EFFICIENCY AND STABILITY OF FORMED CARBONATE MINERALS

TEOH HOU JIE

UNIVERSITI TUNKU ABDUL RAHMAN

OPTIMIZING TEMPERATURE PARAMETERS FOR ENHANCED MINERALIZATION PROCESS: MAXIMIZING CO₂ CONVERSION EFFICIENCY AND STABILITY OF FORMED CARBONATE MINERALS

TEOH HOU JIE

A project report submitted in partial fulfilment of the requirements for the award of Bachelor of Civil Engineering with Honours

Lee Kong Chian Faculty of Engineering and Science Universiti Tunku Abdul Rahman

April 2024

DECLARATION

I hereby declare that this project report is based on my original work except for citations and quotations which have been duly acknowledged. I also declare that it has not been previously and concurrently submitted for any other degree or award at UTAR or other institutions.

Signature : 〰️

Name : TEOH HOU JIE

ID No. : 1902375

Date : 24th April 2024

APPROVAL FOR SUBMISSION

I certify that this project report entitled **"OPTIMIZING TEMPERATURE PARAMETERS FOR ENHANCED MINERALIZATION: OPTIMIZING CO_2 CONVERSION EFFICIENCY AND STABILITY OF FORMED CARBOANTE MINERALS"** was prepared by **TEOH HOU JIE** has met the required standard for submission in partial fulfilment of the requirements for the award of Bachelor of Civil Engineering with Honours at Universiti Tunku Abdul Rahman.

Approved by,

Signature   :

Supervisor   :   Ir Ts Dr Lee Foo Wei

Date   :   29th April 2024

Signature   :

Co-Supervisor   :

Date   :

The copyright of this report belongs to the author under the terms of the copyright Act 1987 as qualified by Intellectual Property Policy of Universiti Tunku Abdul Rahman. Due acknowledgement shall always be made of the use of any material contained in, or derived from, this report.

ACKNOWLEDGEMENTS

I would like to thank everyone who had contributed to the successful completion of this project. I would like to express my gratitude to my research supervisor, Dr. Lee Foo Wei for his invaluable advice, guidance and his enormous patience throughout the development of the research.

In addition, I would also like to express my gratitude to my loving parents and friends who had helped and given me encouragement.

ABSTRACT

The escalating global warming crisis, exacerbated by increasing carbon dioxide (CO_2) emissions and subsequent greenhouse effects, highlights the urgent need for innovative environmental technologies. Industrial processes, like steel production, greatly add to the buildup of industrial waste, increasing environmental worries and requiring new management methods. In this context, mineralization emerges as a promising method addressing both the mounting industrial waste and the imperative to reduce CO_2 emissions. This study investigates the impact of varying temperatures on the mineralization process, utilizing analytical tools such as Scanning Electron Microscopy (SEM), Energy-Dispersive X-ray Spectroscopy (EDX), X-ray Diffraction (XRD) analysis, and Thermogravimetric Analysis (TGA) for comprehensive analysis. Through this investigation, temperature parameters for mineralization are optimized, resulting in the maximization of CO_2 conversion efficiency and determination of thermal stability in the formed carbonate minerals. Local Electric Arc Furnace (EAF) slags, with particle sizes ranging from 0.8 mm to 2.36 mm and comprising 62.72 % calcium oxide, serve as the primary reacting waste materials. The study encompasses 27 sets of slag samples undergoing mineralization under various simulated conditions, including different CO_2 gas concentrations (10 %, 20 %, and 30 %) and humidity levels (40 %, 60 %, and 80 %) at temperatures of 40 °C, 60 °C, and 80 °C. The study achieves a maximum CO_2 conversion efficiency of 12.79 %, under experimental parameters of 80 °C temperature, 30 % CO_2 gas concentration, and 80 % relative humidity levels. EDX testing demonstrates a positive correlation between temperature parameters and CO_2 conversion efficiency, while SEM testing identifies visible crystal structures in the EAF slag samples only at 80 °C mineralization. XRD confirms the presence of calcium carbonate in all samples, with identified polymorphs including 63 % vaterite and 37 % calcite. TGA indicates a 2 % reduction in the sample mass of the carbonate minerals formed when subjected to heating up to approximately 900 °C. In conclusion, this study underscores the pressing need for innovative environmental technologies in combating the escalating global warming crisis.

TABLE OF CONTENTS

LIST OF TABLES

LIST OF FIGURES

LIST OF SYMBOLS / ABBREVIATIONS

wt   Weight Percentage, %

ACC   Amorphous Calcium Carbonate

BSE   Backscattered Electrons

CCS   Carbon Capture and Storage

CCU   Carbon Capture and Utilization

EAF   Electric Arc Furnace

EDX   Energy-Dispersive X-Ray Spectroscopy

DC   Direct Carbonation

IC   Indirect Carbonation

MC   Mineral Carbonation

RH   Relative Humidity, %

SE   Secondary Electrons

SEM   Scanning Electron Microscopy

TGA   Thermogravimetric Analysis

XRD   X-Ray Diffraction

CHAPTER 1

INTRODUCTION

1.1   General Introduction

Carbon Dioxide Capture and Storage (CCS) is associated with several technologies capturing CO_2 at various stages, including combustion for power generation, cement manufacturing, iron and steel production, and natural gas treatment (Sanna, et al., 2014). Then, the captured CO_2 is pressurised before being transported to a storage facility, where it is injected into stable geological sites, and it will be trapped for thousands of years. CCS is not a novel concept, and numerous CO_2 capture technologies are being developed. According to the research by Rahmanihanzaki and Hemmati (2022), although the CCS process is still being developed and reviewed, the main issues remain. There is notable progress in converting carbon dioxide into a valuable resource, bypassing the challenges associated with the CCS method and providing numerous economic benefits. This innovative approach is known as Carbon Capture and Utilisation (CCU). The primary reasons for CCU becoming more appealing than CCS include concerns regarding the long-term storage of carbon, the substantial expenses associated with monitoring, and the lack of profitability.

Mineralization, also known as mineral carbonation, is the reaction that occurs when metal oxide-bearing materials react with CO_2 to form stable carbonate minerals. This reaction can occur either below (in-situ) or above (ex-situ) the ground. It is gaining traction as a potential technology solution for sequestering CO_2 from small and medium-sized emitters where geological sequestration is not feasible (Sanna, et al., 2014). According to Chang, et al. (2017), geological storage, also known as in-situ mineral carbonation, is the most viable option for large-scale storage in which CO_2 is injected into underground reservoirs containing alkali or alkaline earth metals present in the geological formation. However, geological CO_2 poses several uncertainties that must be addressed; bearing the brunt is the potential leakage of injected CO_2.

Unlike in-situ mineral carbonation, ex-situ mineral carbonation encompasses chemical procedures conducted above the Earth's surface. These processes entail reactions between carbon dioxide (CO_2) and alkaline earth

metals like calcium or magnesium. These metals are sourced from naturally occurring silicate minerals, industrial by-products, or industrial wastes. Ex-situ mineral carbonation can be further classified into direct and indirect carbonation. Both methods have been developed into various techniques, including direct gas-solid carbonation, direct aqueous carbonation, multi-stage gas-solid carbonation, indirect aqueous carbonation, the pH swing process, and others. These methods vary based on the specific reactions and materials involved in the processes.

It is worth noting that various factors can vary significantly within direct and indirect carbonation methods. These factors include reaction temperature, reaction time, CO_2 concentration, relative humidity (RH), pH value, and the use of additives. The specific values of these factors may differ depending on the carbonation method or process being employed. These varying factors can lead to differences in CO_2 conversion efficiency and the stability of the resulting products. This is because factors such as reaction rate, solubility, and product formation are dependent on these varying conditions. Additionally, modern tools, including X-ray diffraction (XRD), scanning electron microscopy (SEM), and thermogravimetric analysis (TGA), can be utilised to analyse the CO_2 conversion efficiency of the mineral carbonation process under controlled conditions.

1.2   Importance of the Study

This research aims to contribute to developing effective carbon capture and utilisation (CCU) technologies by optimising temperature parameters in mineralization process to maximise the CO_2 conversion efficiency and the stability of formed carbonate minerals. Maximising the CO_2 conversion efficiency and stability of formed carbonate minerals through temperature optimisation is of paramount importance in addressing environmental impact for several reasons. By enhancing CO_2 conversion efficiency and stability, more carbon dioxide can be effectively removed from the atmosphere and safely stored in stable carbonate minerals. This contributes to mitigating the greenhouse effect and combating climate change.

Following that, enhancing CO_2 conversion efficiency, and ensuring the stability of formed carbonate minerals offer a powerful means of removing

carbon dioxide effectively from the atmosphere. These stable carbonates act as a reliable long-term carbon sink, playing a vital role in mitigating the greenhouse effect and combating climate change. Moreover, carbon capture and mineral carbonation processes provide a practical avenue for capturing CO_2 emissions originating from industrial and energy production sources. The optimisation of temperature parameters enhances the overall effectiveness of these processes, ultimately leading to a notable reduction in greenhouse gas emissions.

Temperature optimisation in mineralization processes also yields substantial economic benefits. Industries can streamline their operations, reduce costs, and shorten the time required for CO_2 conversion. These economic advantages make mineralisation processes more attractive for widespread adoption and implementation, potentially accelerating the transition to a low-carbon economy. Furthermore, temperature optimisation reduces the energy input necessary for carbonation reactions, resulting in enhanced energy efficiency and environmental friendliness. Reduced energy consumption translates into decreased reliance on fossil fuels for process heat, leading to further reductions in emissions. Lastly, this research holds great significance in the realm of waste recycling and converting industrial waste materials into value-added products.

Lastly, mineralization processes enable the recycling and transformation of industrial waste into valuable carbonate minerals. This approach reduces the burden on landfills and converts waste materials into valuable resources, fostering the development of a circular economy and sustainable waste management practices.

1.3   Problem Statement

In recent years, increasing CO_2 emissions from various human activities have resulted in the pressing challenge of climate change, primarily driven by greenhouse gas concentrations. Effective carbon capture and storage (CCS) technologies are critical in combating this issue. Mineral carbonation, the process of converting CO_2 into stable carbonate minerals, has the potential to be a viable CCS strategy. However, to maximise its potential, the mineralisation process must be optimised. Understanding the impact of various parameters on

the mineralisation process, such as temperature, is critical for optimising CO_2 conversion efficiency and facilitating long-term carbon sequestration.

Furthermore, the growing production of industrial wastes such as slags raises environmental concerns while posing significant waste storage and management costs. To address these issues, it is critical to investigate the possibility of using these industrial by-products as feedstock in the carbon mineralisation process. By combining waste utilisation and CO_2 capture, an innovative and environmentally friendly approach emerges, allowing for the reduction of CO_2 emissions while also improving industrial waste disposal practices.

Aside from in-situ mineral carbonation, which directly injects CO_2 into geological formations and has the potential for long-term CO_2 storage, there is significant concern about potential CO_2 leakage back into the atmosphere. Due to its advantages in reducing leakage risks, ex-situ mineral carbonation is a promising CCS technique to address this concern. This method captures and converts CO_2 into carbonate minerals above ground in controlled and confined environments. The stability and durability of formed carbonate minerals are evaluated under optimised temperature and CO_2 conversion conditions to ensure the safety and effectiveness of carbon mineralisation as a secure carbon sequestration method. Understanding the behaviour of these carbonate minerals provides critical insights into the viability and efficacy of ex-situ mineralization as a long-term and dependable carbon-sequestration solution.

1.4   Aim and Objectives

This study aims to determine the optimal temperature influencing the mineralization process, aiming for maximized CO_2 conversion efficiency and thermally stable formation of carbonate minerals. The specific objectives of the study are as follows:

(i)   To investigate the effect of different temperatures on the mineralization process.

(ii)   To identify the maximized CO_2 conversion efficiency of the mineralization process under varying conditions.

(iii)   To determine the thermal stability of the carbonate minerals that formed under the optimized temperature and CO_2 conversion conditions.

1.5   Scope and Limitation of the Study

This study primarily aims to determine the optimal temperature for maximising CO_2 conversion efficiency and evaluating the thermal stability of carbonate minerals formed. Electric Arc Furnace (EAF) slag, with a particle size range of 0.8 mm to 2.36 mm, acts as the reactant material with CO_2 gas in the mineralization process in this study. Prior to mineralization, the EAF slag undergoes mechanical pretreatment for standardisation, wherein 10g of the material is compacted into a cylinder measuring 20mm in diameter and 10mm in height using a hydraulic compaction machine.

The temperature parameters for mineralization range from 40 °C to 80 °C, with increments of 20 °C. In this study, the mineralization process is conducted for a duration of 24 hours and under various simulated conditions, including different relative humidity levels (40 %, 60 %, and 80 %) and concentrations of CO_2 (10 %, 20 %, and 30 %). This ensures consistency in temperature effects across diverse conditions, resulting in a total of 27 sets of carbonated samples. In addition, the CO_2 conversion efficiency and thermal stability of the carbonate minerals formed are assessed using analytical methods such as Scanning Electron Microscopy (SEM), Energy-Dispersive X-ray spectroscopy (EDX), X-ray diffraction (XRD) analysis, and Thermogravimetric Analysis (TGA).

However, this study faces certain limitations. Firstly, the mineral carbonation chamber is limited to a maximum temperature of 99.9 °C and a maximum CO_2 concentration of 30 %. Moreover, due to constraints in laboratory resources and limited time, each of the 27 sets of samples will only undergo the mineralization process and laboratory tests once, resulting in a single set of results. Furthermore, out of the 27, only 9 of them will undergo TGA for thermal analysis. These 9 samples encompass varying temperature parameters (40 °C, 60 °C, and 80 °C), different CO_2 concentrations (10 %, 20 %, and 30 %), and a consistent relative humidity of 40 %.

1.6   Contribution of the Study

This study makes a significant contribution to the field by systematically exploring temperature parameters to optimize the mineralization process, aiming to maximise CO_2 conversion efficiency and ensure the stability of formed carbonate minerals. Through a comprehensive investigation, the study sheds light on the intricate relationship between temperature conditions and mineralization dynamics. Notably, the positive correlation observed between temperature parameters and CO_2 conversion efficiency provides valuable insights into the temperature-dependent reactions governing the mineralization process.

By identifying the maximised CO_2 conversion efficiency under specific experimental conditions, the study offers practical guidance for optimizing mineralization processes to achieve maximum CO_2 capture and utilization. Furthermore, the detailed characterization of formed carbonate minerals using advanced analytical techniques such as Energy-Dispersive X-ray Spectroscopy (EDX), Scanning Electron Microscopy (SEM), and X-ray Diffraction (XRD) analysis enhances our understanding of mineral formation processes. Identifying calcium carbonate polymorphs and assessing their stability contribute to the development of sustainable practices by evaluating the long-term viability of carbon capture and utilization strategies.

Overall, the findings of this study have implications for the advancement of sustainable solutions to mitigate greenhouse gas emissions and promote the utilization of CO_2 as a valuable resource in various industrial applications. This research represents a significant step towards optimizing

mineralization processes and advancing our understanding of CO_2 conversion efficiency and the stability of formed carbonate minerals. Ultimately, these insights contribute to the development of innovative strategies for addressing climate change challenges and transitioning towards a more sustainable future.

1.7   Outline of the Report

This report consists of five chapters aiming to deliver a comprehensive study on optimizing temperature parameters to enhance the mineralization process, aiming to maximise CO_2 conversion efficiency and ensure the stability of formed carbonate minerals.

In Chapter 1, an overview of the study is presented, covering the introduction, importance of the study, and problem statement. Additionally, it outlines the aims and objectives, scope and limitations, and the contribution of the study.

Chapter 2 delves into the literature review to provide a deeper understanding related to the study. This includes mineral carbonation and its reaction mechanism, potential factors influencing the mineralization process, suitable feedstock for mineralization, explanation of crystalline polymorphs of carbonate minerals, stability of formed carbonate minerals, and analytical methods utilized in the study.

Chapter 3 describes the methodology and work plan, including raw materials preparation, pre-treatment, and mineralization of EAF slag samples. This section includes conducting four laboratory tests to analyse the carbonated EAF slag samples following mineralization. The four tests are: Scanning Electron Microscopy (SEM), Energy-Dispersive X-ray Spectroscopy (EDX), X-ray Diffraction (XRD) analysis, and Thermogravimetric Analysis (TGA).

Chapter 4 presents the results obtained from the laboratory tests and discusses the analysed findings. Qualitative observations and quantitative measurements are recorded and presented in tables and graphs to illustrate the effect of temperature on the mineralization process. This aids in determining the optimized temperature and evaluating the thermal stability of the formed carbonate minerals.

Finally, Chapter 5 summarizes the findings of the study in relation to the objectives outlined at the outset. It provides valuable insights into the effect of temperature on the mineralization process and determines the maximized CO_2 conversion efficiency and thermal stability of formed carbonate minerals.

CHAPTER 2

LITERATURE REVIEW

2.1 Introduction

This chapter offers an extensive overview of various mineralization methods, potential factors influencing mineralization, the reaction mechanisms mineralization, appropriate feedstock, stability of carbonate mineral formed, and relevant analytical methods. The literature review aims to illustrate how temperature can potentially impact the optimisation of CO_2 conversion efficiency and the stability of carbonate mineral formed.

2.2 Mineral Carbonation

Carbon sequestration through mineral carbonation is a process that involves the conversion of CO_2 into stable carbonate minerals. This occurs naturally through the weathering of rocks when CO_2 dissolves in rainwater and reacts with alkaline minerals. Two main approaches to implementing mineral carbonation exist: in situ mineral carbonation and ex-situ mineral carbonation (Xiao, et al., 2019).

In situ carbonation entails injecting CO_2 underground surface, whereas ex-situ carbonation occurs above ground surface utilising minerals. The utilisation of subsurface alkalis in this method may entail significant energy and cost expenditures, along with environmental issues linked to extraction. Conversely, industrial residues are frequently well-suited for carbonation and are easily accessible. Generally, industrial residues demonstrate greater reactivity in comparison to natural minerals (Rahmanihanzaki and Hemmati, 2022).

Ex-situ mineral carbonation can be achieved through both direct (gas-based and aqueous-based) and indirect processes. Figure 2.1 provides an overview of the fundamental principles underlying these direct and indirect processes. In the direct process, CO_2 directly reacts with minerals to form carbonates in a single step. In contrast, the indirect process involves the prior extraction of alkaline earth metal oxides, such as calcium oxide (CaO) and magnesium oxide (MgO), before the carbonation step (Xiao, et al., 2019).

Furthermore, Figure 2.2 illustrates an overview of various mineral carbonation methods involving both direct and indirect mineral carbonation.
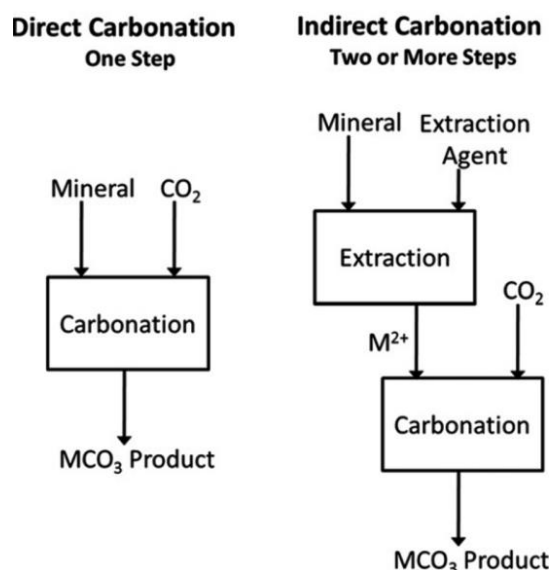
Figure 2.1: General Overview of Mineral Carbonation (Azdarpour, et al., 2015).
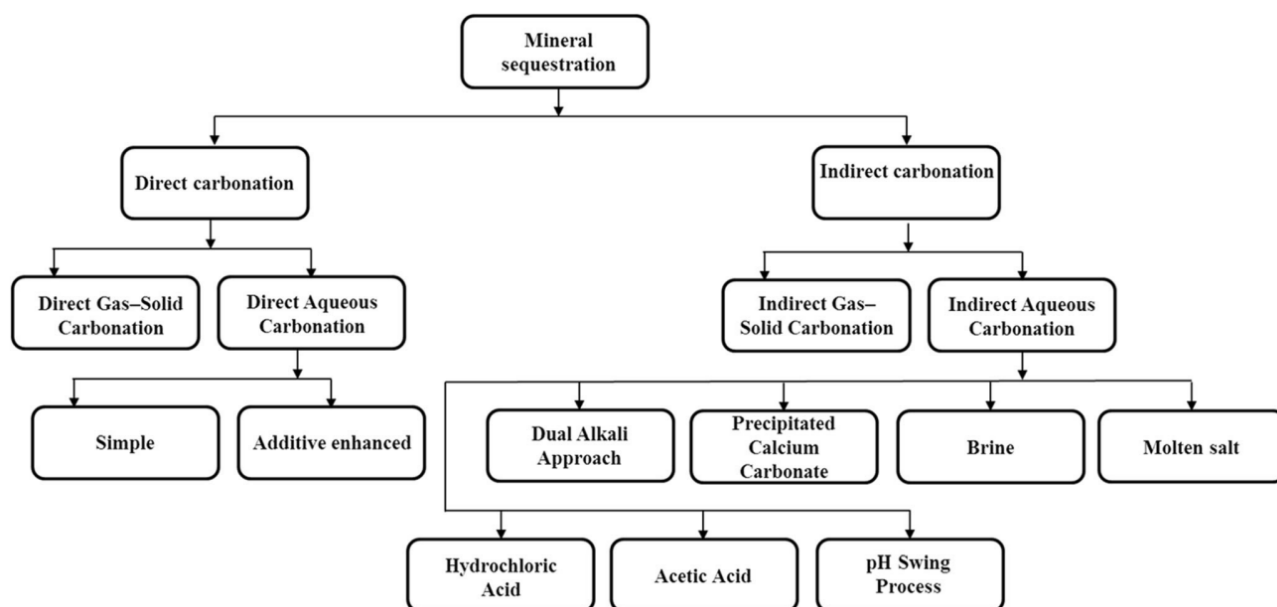
Figure 2.2: Summary of Mineral Carbonation Methods (Yadav and Mehra, 2021).

The processes involved in mineral carbonation can be divided into separate phases: initially, the dissolving of CO_2 in the liquid phase; secondly, the formation of divalent ions from the mineral structure; and lastly, the formation

of carbonates. It is crucial to emphasise that the dissolution of alkaline solids serves as a bottleneck, limiting the supply of cations needed for carbonate precipitation (Rahmanihanzaki and Hemmati, 2022). Various factors have the potential to influence carbonation, including carbonation time, reaction temperature, CO_2 concentration, particle size, pressure, moisture levels, humidity, additives, and several others.

2.2.1 Direct Carbonation

Direct carbonation (DC) has two methods: direct gas-solid carbonation and direct aqueous carbonation. Direct carbonation can be additionally classified into two types: with pre-treatments and without pre-treatments (Sanna, et al., 2014). According to Yadav and Mehra (2021), direct routes are typically designed. Nonetheless, these methods often necessitate elevated CO_2 pressure and temperature levels, which can lead to slower reaction rates and lower conversion rates. Various physical and chemical preparatory steps and mechanical and thermal activation can be employed to enhance mineral reactivity. By augmenting the surface area, these pre-treatments have the potential to enhance reaction rates and overall efficiency. However, chemical pre-processing, among other factors, can reduce magnesium oxide (MgO) content, consequently reducing the mineral's capacity for carbonation. Additionally, direct methods tend to demand significant amounts of energy, indirectly releasing more carbon dioxide (CO_2) emissions than the process can sequester.

2.2.1.1 Direct Gas-Solid Carbonation

Gas-solid carbonation is the simplest and most basic approach to carbonation. It involves a one-step process whereby pure CO_2 gas interacts with substances containing calcium and magnesium oxides, forming carbonates. This reaction is both exothermic, releasing heat, and slow, and the sluggish pace of the reaction presents a notable obstacle for the direct carbonation technique. Several approaches have been explored to address this issue and enhance the reaction kinetics. These include mineral pre-activation and the application of elevated temperature and pressure. However, these methods introduce complexity to the reaction process and result in higher energy consumption, potentially diverting

from the primary objective of reducing CO_2 emissions into the atmosphere. Additionally, the end products generated through this method often have a low added value. There are two methods to accelerate the reaction rate (Rahmanihanzaki and Hemmati, 2022):

(i)   Conducting the carbonation with the presence of water or water vapour.

(ii)   The reaction is conducted indirectly in multi-stages.

As an example, the direct gas-solid reaction of olivine is given as in Eq.2.1 (Sanna, et al., 2014):

$$Mg_2SiO_{4(s)} + 2CO_{2(g)} \rightarrow 2MgCO_{3(s)} + SiO_{2(s)} \qquad (2.1)$$
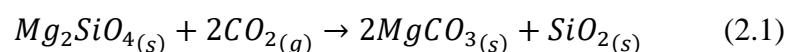
2.2.1.2   Direct Aqueous Carbonation

The main objective of aqueous reactions is to create conditions that allow the reaction of relevant alkali metal oxides and CO_2 in the presence of water or water vapour. One of the primary advantages of using water or steam in these reactions is the ability to accelerate mineralisation under mild conditions, as opposed to solid-gas processes. Furthermore, feedstock properties, reaction temperature, pressure, and CO_2 concentration considerably impact final efficiency and utilisation capacity. During the carbonation process, there is a strong emphasis on reducing energy consumption while maximising CO_2 utilisation (Zhang, et al., 2020).

Due to lower operating temperatures and pressures, Rahmanihanzaki and Hemmati (2022) outlined that aqueous carbonation is preferred over gas-solid reactions. The addition of specific chemicals can also improve it. Aqueous carbonation can be completed in a single or two-step process. The processes involved in mineral carbonation are categorised into three distinct stages: first, the dissolution of CO_2 in the aqueous phase; second, the precipitation of divalent ions from the mineral matrix; and finally, the deposition of carbonates. It is crucial to emphasise that the dissolution of alkaline solids represents a critical bottleneck in the availability of cations required for carbonate precipitate formation. For instance, the reactions associated with the three-step mechanism

of direct aqueous carbonation for olivine are illustrated below (Yadav and Mehra, 2021):

(i)   The leaching of minerals, as shown in Eq.2.2.

(ii) The dissolution of CO_2 followed by the release of carbonate ions, as shown in Eq.2.3.

(iii) The nucleation and growth of carbonate minerals, as shown in Eq.2.4.

$$Mg_2SiO_{4(s)} + 4H^+_{(aq)} \rightarrow 2Mg^{2+}_{(aq)} + 2H_2O_{(l)} + SiO_{2(s)} \quad (2.2)$$

$$CO_{2(g)} + H_2O_{(l)} \rightarrow CO_3{}^{2-}_{(aq)} + 2H^+_{(aq)} \quad (2.3)$$

$$Mg^{2+}_{(aq)} + CO_3{}^{2-}_{(aq)} \rightarrow MgCO_{3(s)} \quad (2.4)$$
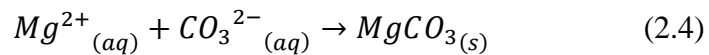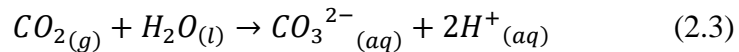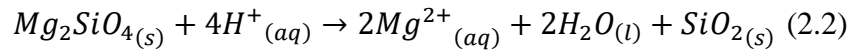
This three-step process occurs simultaneously within a single reactor. First, CO_2 dissolves in water, creating carbonic acid (H_2CO_3), which releases hydrogen ions (H^+) and bicarbonate ions (HCO^{3-}) due to the instability of the acid. An equilibrium between H^+ and CO_3^{2-} is established through the dissolution of bicarbonate acid in water. The presence of H^+ initiates the hydrolysis of minerals, releasing magnesium ions (Mg^{2+}) and silica (SiO_2). Consequently, with the presence of free protons, the pH of the solution decreases, resulting in an acidic environment. This acidity creates favourable conditions for the dissolution of alkalis. Additionally, an increase in pressure can accelerate the rate of pH reduction. With increased pressure, the quantity of dissolved CO_2 also rises, releasing higher number of protons and causing a further reduce in pH. Subsequently, the Mg^{2+} and HCO^{3-} ions react to form solid carbonate (Yadav and Mehra, 2021).

Yadav and Mehra (2021) point out that mineral dissolution represents the most time-consuming phase in the reaction. However, its kinetics can be accelerated through the facilitation of silicate dissolution with the introduction of additives and adjustments in operational parameters. Modifying conditions can be accomplished by changing factors such as temperature, the ratio of solids to liquids, CO_2 concentration, pressure, and particle size. Moreover, the inclusion of chemicals like acids, bases, or salts as additives can expedite the reaction process. Acids and complexing agents like HCl, CH_3COOH, and

formic acid (HCOOH) are reaction accelerators. Furthermore, alkali metal hydroxides can be used to improve the chemistry of the solution even further. These not only enhance CO_2 absorption but also raise the pH of the solution without depleting the hydroxide. Both HCO^{3-} and OH^- ions act as catalysts. Another method to boost both the dissolution of Mg_2SiO_4 and the elevation of pH is by adding Na_2CO_3. Salt additives such as NaCl, sodium bicarbonate ($NaHCO_3$), and $NaNO_3$ or KNO_3 can expedite the reaction by increasing the ionic strength of the solution. This reduction in the Ca/Mg activity within the solution promotes the release of Mg^{2+} and Ca^{2+} ions from the minerals. The reaction mechanism for the dissolution of Mg_2SiO_4 by adding $NaHCO_3$ and Na_2CO_3 is illustrated as follows (Eq.2.5 to Eq.2.7):

$$NaHCO_{3(s)} \rightarrow Na^+{}_{(aq)} + HCO_3{}^-{}_{(aq)} \qquad (2.5)$$

$$Mg_2SiO_{4(s)} + 4Na^+{}_{(aq)} + 4HCO_3{}^-{}_{(aq)} \qquad (2.6)$$
$$\rightarrow 2MgCO_{3(s)} + SiO_{2(s)} + 2Na_2CO_{3(aq)} + 2H_2O_{(l)}$$

$$Na_2CO_{3(aq)} + H^+{}_{(aq)} + HCO_3{}^-{}_{(aq)} \rightarrow 2NaHCO_{3(s)} \qquad (2.7)$$
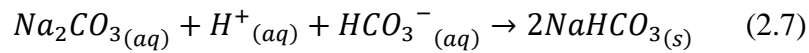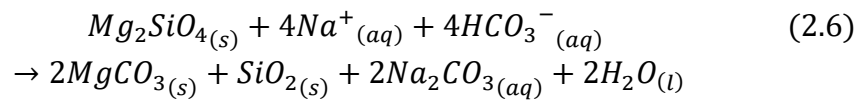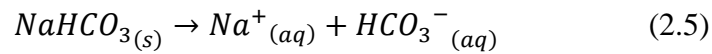
$NaHCO_3$, when introduced, increases the concentration of HCO^{3-}, consequently accelerating the reaction rate. Its addition slightly alkalises the solution, elevating the pH from 7.7 to 8.0. The pH level in the solution critical in reaction kinetics. A higher pH is an efficient vehicle for CO_2 and reduces reaction time. The interaction between hydroxyl ions and gaseous CO_2 leads to almost instantaneous bicarbonate regeneration. Consequently, this approach keeps the HCO^{3-} concentration and pH in the solution stable, and there is no depletion of $NaHCO_3$ during the procedure. Furthermore, certain salt additives create complexes with the dissolved Mg and Ca, diminishing their reactivity in the solution, thereby leading to an enhanced release of Mg and Ca ions from the silicate minerals (Yadav and Mehra, 2021).

2.2.2 Indirect Carbonation

The indirect carbonation (IC) route typically encompasses a multi-step process, encompassing the extraction of Ca or Mg components as the first step, followed by a precipitation reaction between Ca/Mg and CO_2 in either gaseous or aqueous

phases as the second step (Chang, et al., 2017). According to Azdarpour, et al. (2015), this approach can be applied in a variety of ways, including indirect multistage gas-solid mineral carbonation, the pH swing process, HCl extraction, the molten salt process, alternative acid extraction techniques, and ammonia extraction. Even though the carbonation rate is higher in aqueous carbonation when using NaOH, NaCl, $NaHCO_3$, $KHCO_3$, etc., compared to gas-solid reactions, achieving the required conversion rates still necessitates certain modifications. The factors such as mineral dissolution, control of product layer diffusion to mitigate CO_2 diffusion, and CO_2 dissolution make direct mineral carbonation impractical for commercial advancement. Because the indirect carbonation process dissociates the precipitation step from the dissolution of raw materials, it is expected that the carbonate minerals of greater purity will result when compared to the direct carbonation route (Chang, et al., 2017). Furthermore, the calcium and magnesium conversion rate to carbonates is considerably greater with indirect methods. Breaking down the direct gas-solid mineral carbonation route into multiple steps could enhance the conversion rate. However, indirect gas-solid mineral carbonation requires a substantial heat input, leading to inherent energy losses. Thus, indirect aqueous mineral carbonation solves the challenges associated with direct and indirect gas-solid mineral carbonation (Azdarpour, et al., 2015). There are several indirect aqueous mineral carbonation methods, including the acid leaching process, molten salt process, and pH-swing process.

2.2.2.1 Acid Leaching Process

According to Xiao, et al. (2019), many acids, including hydrochloric acid (HCl), nitric acid (HNO_3), and acetic acid (CH_3COOH), can extract the reactive component from feedstock minerals. For example, to extract Mg from serpentine, the typical HCl extraction process is proposed, which can be divided into three steps, as shown in Eq.2.8 to Eq.2.10. The initial stage of the process involves the extraction of minerals using HCl. Subsequently, the solution is heated to a temperature that vaporises water, leading to the precipitation of $Mg(OH)_2$ and the recovery of HCl. The resulting $Mg(OH)_2$ is dissolved in water and permitted to react with CO_2 to form $MgCO_3$. According to Huijgen and Comans (2005a), the reactions are illustrated as follows (Eq.8 to Eq.11):

$$Mg_3Si_2O_5(OH)_{4(s)} + 6HCl_{(l)} + H_2O_{(l)} \rightarrow 3MgCl_2 \cdot 6H_2O_{(aq)} + SiO_{2(s)} \quad (2.8)$$

$$MgCl_2 \cdot 6H_2O_{(aq)} \rightarrow MgCl(OH)_{(l)} + HCl_{(l)} + 5H_2O_{(l)} \quad (2.9)$$

$$2MgCl(OH)_{(l)} \rightarrow Mg(OH)_{2(s)} + MgCl_{2(l/s)} \quad (2.10)$$

$$Mg(OH)_{2(s)} + CO_{2(g)} \rightarrow MgCO_{3(s)} + H_2O_{(aq)} \quad (2.11)$$
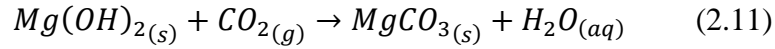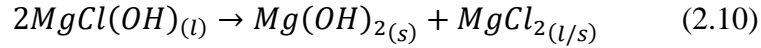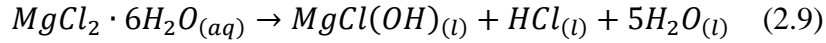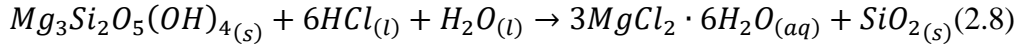
However, the costs associated with using HCl as well as energy consumed by the H₂O evaporation step are significant drawbacks of this approach. The energy consumed by the process's dehydration and crystallisation steps was four times greater than the energy produced by the power station emitting CO₂ (Huijgen and Comans, 2005a). Furthermore, the existence of soluble chloride near alkali metals triggers the creation of alkali metal chlorides, which poses challenges for HCl recovery and leads to undesirable HCl losses. Additionally, the desired quantity of alkali metals in the feedstock is typically less than 1 % by weight. Regrettably, solid waste materials often contain a higher concentration of alkali metals. Consequently, this approach is not a feasible option for mineral sequestration from alkaline solid waste (Yadav and Mehra, 2021).

2.2.2.2 Molten Salt Process

According to Xiao, et al. (2019), the molten salt extraction process was proposed to reduce the high cost of acid extraction. Molten salts such as alkali metal nitrates and alkali earth metal carbonates have numerous benefits, including thermodynamic stability at high temperatures, low pressure at operating temperatures, and a broad range of solubility (Shen, 2023). Generally, magnesium chloride (MgCl₂) will be utilised as an extraction agent to extract magnesium from serpentine, and the reaction is as follows (Eq.2.12 to Eq.2.15):

$$2MgCl(OH)_{(aq)} + nH_2O_{(aq)} \rightarrow MgCl_{2(aq)} \cdot nH_2O_{(aq)} + Mg(OH)_{(s)} \quad (2.13)$$

$$MgCl_2 \cdot nH_2O \rightarrow MgCl_2 \cdot 3.5H_2O_{(l)} + (n - 3.5)H_2O \quad (2.14)$$

$$Mg(OH)_{2(s)} + CO_{2(g)} \rightarrow MgCO_{3(s)} + H_2O_{(aq)} \quad (2.15)$$
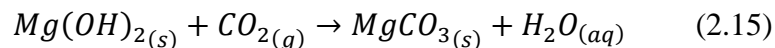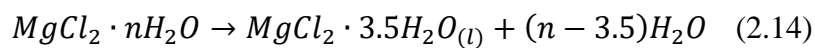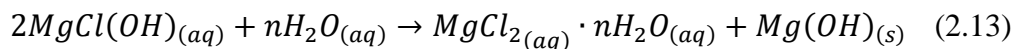
First, serpentine is dissolved in molten salt. Then, silica precipitates at a temperature around 150 °C. Following that, water is added, causing magnesium hydroxide (Mg(OH)$_2$) to precipitate. Afterwards, MgCl$_2$ is partially dehydrated to recover the solvent within a temperature range of 110 °C to 250 °C. In the final step, magnesium hydroxide is separated and subjected to carbonation (Huijgen and Comans, 2005a).

2.2.2.3 pH-Swing Process

The pH swing process is a two-step indirect aqueous carbonation process (Yadav and Mehra, 2021). According to Azdarpour, et al. (2014), adding acids and bases during the pH swing process in the first and second steps can improve Ca/Mg extraction and carbonate precipitation rates. Adding acid to the solution lowers the pH, improving the metal ion extraction rate. In the second step, the addition of bases raises the pH of the solution, resulting in increased carbonation and precipitation. The optimal pH for aqueous carbonation is estimated to be around 10. Wang and Maroto-Valer (2011) stated a novel pH-swing mineral carbonation method that uses recyclable ammonium salts. Ammonium salts, including ammonium nitrate (NH$_4$NO$_3$), ammonium chloride (NH$_4$Cl), and ammonium acetate (CH$_3$COONH$_4$) can be used to extract Ca or Mg from industrial waste such as steel slag (Jo, et al., 2014).

The modified process diagram is illustrated in Figure 2.3. In this process, aqueous ammonium bisulphate (NH$_4$HSO$_4$) was used to extract Mg from serpentine. Subsequently, the solution's pH was modified by introducing aqueous ammonia, which led to the precipitation of iron and silicon from the solution. Following that, ammonium bicarbonate (NH$_4$HCO$_3$) and ammonia (NH$_3$) solutions were introduced to react with Mg, producing carbonates and ammonium sulphate ((NH$_4$)$_2$SO$_4$), which were recycled through evaporation and decomposed back into NH$_3$ and NH$_4$HSO$_4$ (Wang and Maroto-Valer, 2011).
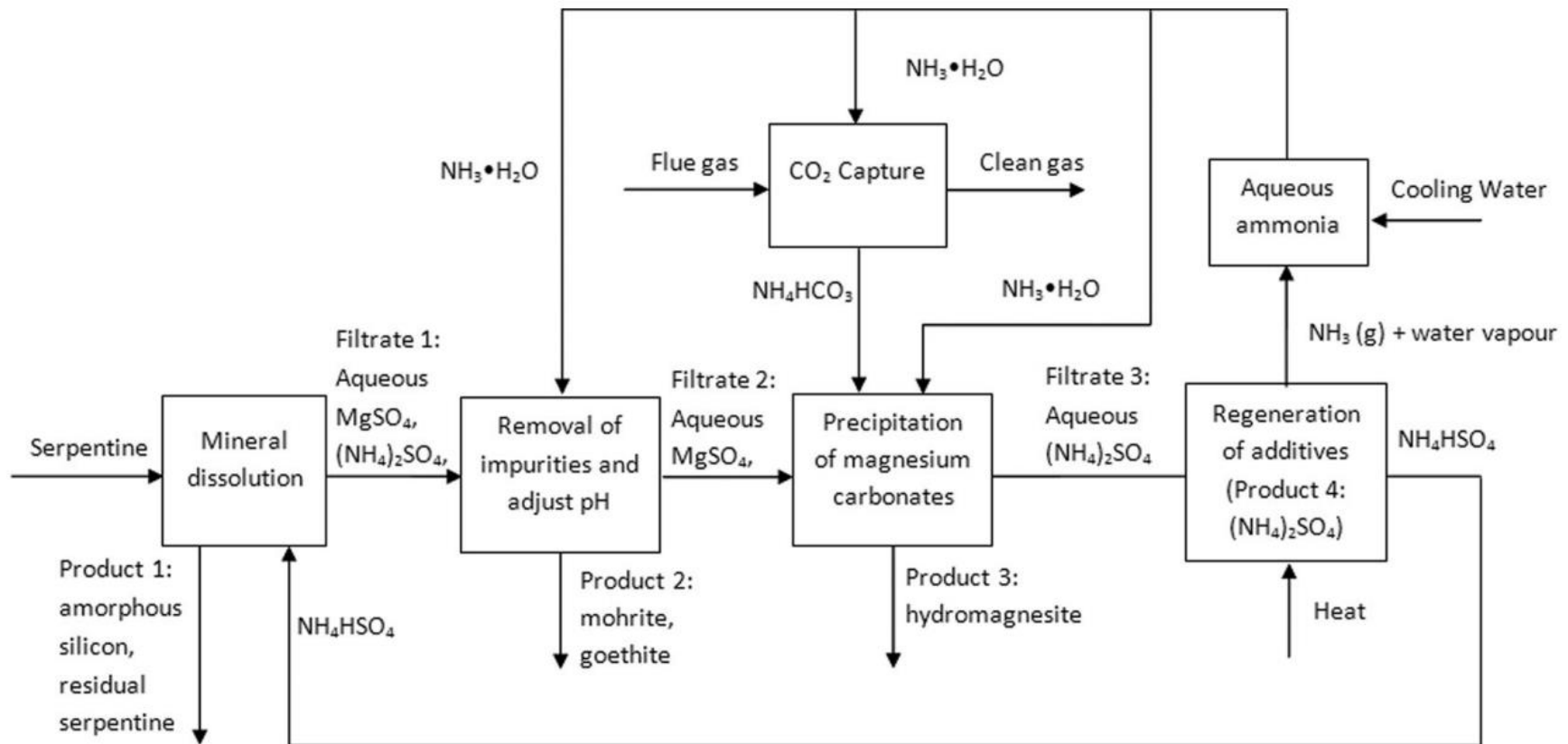
Figure 2.3: Improved Reaction Route of pH-Swing CO_2 Mineral Sequestration with Reusable Ammonium Salts (Wang and Maroto-Valer, 2011).

2.3   Reaction Mechanism

2.3.1   Silicate Weathering

Mineral carbonation involves the reaction of CO_2 with metal oxide-bearing materials to produce insoluble metal carbonates, with calcium and magnesium being the most reactive metals. In the natural world, this process is known as silicate weathering, which occurs over geological time scales. It relies on naturally occurring silicates as sources of alkaline and alkaline-earth metals and acts to sequester atmospheric CO_2 (Abanades, et al., 2005). According to Pan, et al. (2018), silicate weathering is governed by the diffusion of atmospheric CO_2 towards the centre of the minerals because of the lower concentration of CO_2 and moisture in the atmosphere. They have delineated the mechanism, as illustrated in Figure 2.4, into three main stages that regulate the rate of CO_2 absorption:

(i)   **Diffusion**: Gaseous CO_2 diffuses into unsaturated phases through the porous medium.

(ii)   **Dissolution**: Gaseous CO_2 dissolves in interstitial water.

(iii)   **Precipitation**: Metal carbonates precipitate from the interstitial water.
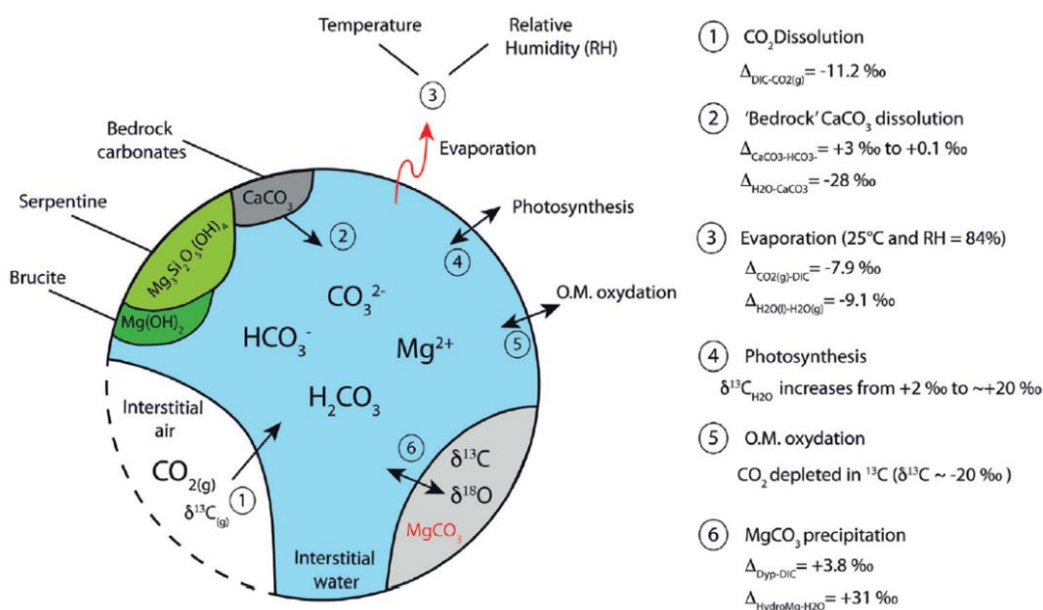
Figure 2.4: A Process-Based Conceptual Model for Carbonation Reaction in Silicate Weathering (Pan, et al., 2018).

2.3.2   Accelerated Carbonation

As outlined by Pan, et al. (2018), the CO_2 mineralisation process employing alkaline solid wastes is characterised as a multifaceted, heterogeneous, and irreversible reaction between fluids and solid particles. This process operates within a dynamic system and involves two interfaces: the gas-liquid and liquid-solid interfaces. The overall reaction can be distilled into three concurrent steps:

(i)   **Dissolution of CO_2**: In this step, CO_2 dissolves into the bulk solution via the gas-liquid interface. Compounds containing CO_2 permeate from the bulk fluid phase with two potential paths: These metal ions may saturate the mineral matrix by entering the micropores and reacting with the reactive components, or they can straightly interact with the reactive components that have leached out from the mineral matrix at the interface between water and the solid. The dissolution of gaseous CO_2 in this context is frequently regarded as a diffusion-limited step, where the exchange of mass between the gas and liquid phases is important in affecting the kinetics of the reaction.

(ii)   **Leaching of Reactive Components**: In this step, reactive components (such as Ca^{2+} or Mg^{2+}) leach from the solid matrix into the solution at the liquid-solid interface. In the process of CO_2 mineralization, Leaching is responsible for dissolving and liberating metal ions from the solid matrix into the aqueous solution, which can include materials such as steel slag or fly ash. The rate at which metal ions are leached out is determined by the mineral composition of the metal oxides in the solid matrix, as well as their attraction or affinity to specific chemical species present in solution and pore water.

(iii)   **Precipitation of Carbonate Crystals**: During this stage, carbonate crystals, such as $CaCO_3$ or $MgCO_3$, can precipitate either within the bulk liquid phase or at the interface between the liquid and solid phases. According to Chiang and Pan (2017), the interaction between Ca^{2+} and CO_3^{2-} ions leads to the

formation of $CaCO_3$ precipitates. It's worth noting that $CaCO_3$ is highly insoluble in water when the pH exceeds 9. The reaction between calcium ions and carbonate ions occurs rapidly and is typically influenced by their concentrations in the liquid phase. Furthermore, it's important to consider changes in particle size during the reaction in practical applications. Particle size can alter because of the formation of ash and/or product layers, which can impact the diffusion of reactants within these layers.

2.4   Potential Factors Affecting Carbonation

Because alkaline solid wastes, such as EAF slags, possess diverse properties, various types of steel slag exhibit varying responses to rapid carbonation. The micro-scale processes associated with steel slag carbonation are greatly impacted by Ca^{2+} dissolution and CO_2 diffusion, which consequently impact the carbonation efficiency. According to the research (Wang, et al., 2021), EAF slags typically has a chemical composition of CaO and MgO of around 38 % and 12 %, respectively. As a result, it possesses an abundance of cations capable of adsorbing more CO_2. The wide range of chemical compositions found in alkaline solid wastes makes it challenging to establish a precise law governing accelerated carbonation. Apart from variations in mineral compositions among different steel slags, there are several factors influencing mineralization process, including reaction time, reaction temperature, CO_2 concentration, particle size, pressure, moisture levels, humidity, additives, and many others, as illustrated in Figure 2.5 (Baras, et al., 2023).
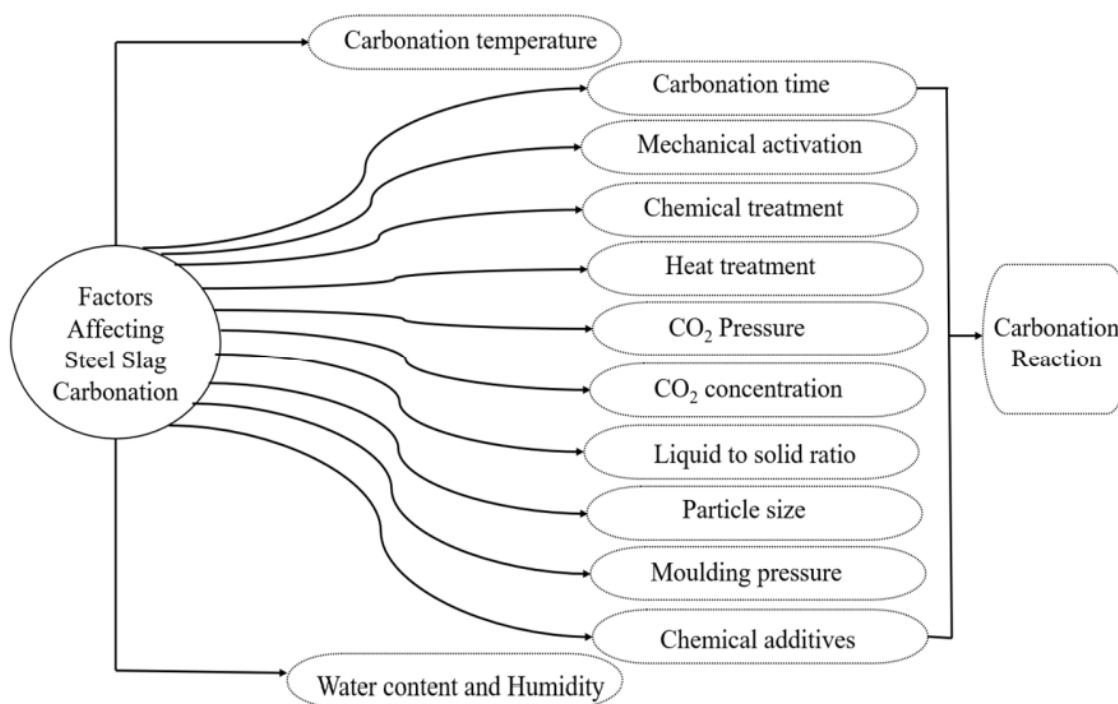
Figure 2.5: Factors Influencing Carbonation Reaction (Baras, et al., 2023).

2.4.1 Reaction Temperature

The mineralization process of steel slag is significantly affected by the temperature at which it is conducted. This factor significantly increases the CO_2 solubility and the rate at which slag dissolves during aqueous carbonation (Baras, et al., 2023). For instance, an experiment involving various temperature conditions applied to different particle sizes of EAF slag carbonation (ranging from 3.5 mm to 7 mm, 7 mm to 15 mm, to 15 mm to 25 mm) has been conducted and demonstrated that elevated temperatures led to improved carbonation reactions, despite with a simultaneous decrease in the water-solubility of CO_2 (Ko, Chen, & Jiang, 2015). Unexpectedly, raising the temperature beyond 200 °C slowed the carbonation rate, indicating that 200 °C was the optimal temperature for this process. This observation was consistent with another study that found 200 °C to be the optimal temperature for the carbonation, enhancing mineral dissolution (Song, et al., 2021).

Notably, the reaction temperature for dry carbonation typically exceeds that of aqueous carbonation (Yu & Wang, 2011). Research conducted by Ghacham, et al. (2016) underscored the significant influence of reaction temperature on the effectiveness of carbonation in suspended steel slag under conditions of high partial pressures of CO_2. It is observed a significant increase in CO_2 conversion efficiency, rising from 46 % to 70 %, as the temperature elevated from 50 °C to 200 °C. However, Liu, Liu, and Qi (2016) discovered that high-temperature curing can have complex effects. While it can enhance the early hydration rate, it may also lead to the formation of large voids and increased cracking in the hardened paste. Additionally, subjecting the material to high-temperature curing can inhibit subsequent hydration reactions, leading to a reduced extent of cementitious material hydration compared to conventional curing approaches. Consequently, carbonation curing may have adverse effects on material properties.

In practical terms, it is advisable to initially elevate the reaction temperature to expedite surface reactions and promote carbonation. However, as the temperature increases, influenced by both CO_2 concentrations and humidity, the internal diffusion rate of CO_2 diminishes, ultimately leading to a reduction in the extent of carbonation (Song, et al., 2021). Additionally, the reaction temperature also affects the location where calcium carbonate forms.

At lower temperatures, most $CaCO_3$ precipitates on the surface of solid and liquid slag due to the high concentration of dissolved CO_2. Conversely, at higher temperatures, increased calcium concentrations dissolved in the liquid phase favour the precipitation of $CaCO_3$ during the interaction between gas and water. These findings collectively emphasise the intricate interplay between temperature and the carbonation process, highlighting the importance of carefully considering and controlling temperature conditions for optimal results in carbonation studies.

2.4.2   Reaction Time

The duration of the mineralization process plays a pivotal role in determining the carbonation depth and strength of steel slags. It is a crucial factor with economic implications in the mineralization of steel slags. As the reaction time increases, so does the carbonation depth and the CO_2 sequestration capacity of steel-making slag (Ghacham, et al., 2016). Carbonation progresses rapidly but gradually slows down, eventually reaching equilibrium (Chen, et al., 2021). Longer carbonation durations, as demonstrated by Huijgen and Comans (2005b), lead to higher carbonation degrees. Interestingly, the carbon fixation response is more rapid in the early stages and gradually stabilises over time. For instance, within the first 2 minutes, 40 % of the calcium undergoes carbonation, with only an additional 13 % reacting over the next 30 minutes. Despite the swift initial carbonation, certain inner regions of EAF concrete specimens remain uncarbonated even after extended carbonation durations. Typically, steel slags display a limited degree of carbonation reactivity, and as a result, $CaCO_3$ particles produced during the process can potentially block the pores of the specimen, considerably hindering the diffusion of CO_2 (Song, et al., 2021).

Wei, et al. (2022) observed that prolonging the reaction duration expedites the mineralization process in steel slag-desulfurization gypsum, eventually reaching equilibrium. Nevertheless, extending the carbonation process does not yield a significantly improved carbonation effect. It's crucial to avoid excessive use of machinery and equipment to prevent resource wastage. The optimal reaction time was determined as 12 hours. The reaction time is also a key indicator in a reactive economy. At a temperature of 80°C, the study investigated the influence of reaction time at intervals of 10 minutes, 20 minutes,

30 minutes, 60 minutes, 90 minutes, and 120 minutes, while maintaining alkali to slag ratios of 0 % and 4 % by weight. Figure 2.6 demonstrates that the slag's capacity to capture CO_2 rises as to the reaction time extends. This enhancement primarily stems from the formation of $CaCO_3$ (Ghacham, et al., 2016). In summary, the duration of the carbonation process emerges as a critical factor influencing both the carbonation depth and the mineralization process effectiveness of steel slags, with implications for resource efficiency and the overall carbonation effect.
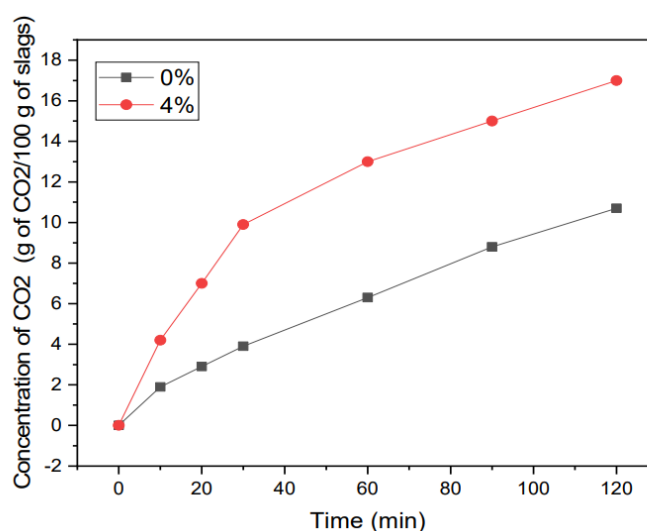
Figure 2.6: Effect of carbonation time (Ghacham, et al., 2016).

2.4.3 CO_2 Concentration

The mineralization efficiency of steel slag is significantly impacted by CO_2 diffusion and dissolution rates within the material. One approach to assessing the carbonation level, as Ko, Chen, and Jiang (2015) demonstrate, involves monitoring pH changes. Their study found that as CO_2 concentration increased, the carbonation degree of EAF steel slag decreased. In a study by Yu and Wang (2011), it was observed that decreasing CO_2 concentrations led to an increased carbonisation reaction rate. This suggests a nuanced relationship between CO_2 concentration and carbonation kinetics. Rađenović, Malina and Sofilić (2013) explored that initially, higher CO_2 levels result in higher mineralization efficiency. However, extending the carbonation duration at lower CO_2

concentrations can lead to equivalent or even higher CO_2 absorption rates compared to higher CO_2 concentrations.

Further insights from Wang, et al. (2020) emphasised the consequence of CO_2 concentration on EAF slag mineralization. Unexpectedly, their research revealed that CO_2 sequestration did not increase with higher CO_2 concentrations. The lowest calcium utilisation was noticed when CO_2 concentrations were set at 50% for both steel slags. Intriguingly, the calcium consumption rate increased at CO_2 concentrations of 10 % to 75 %. This highlights the complex relationship between CO_2 concentration and carbonation efficiency. In addition, Prigiobbe, Polettini, and Baciocchi (2009) noted that the highest calcium conversion was achieved at a CO_2 concentration of 10 % when operating at temperatures of 400 °C to 450 °C. These findings underscore the intricate interplay between CO_2 concentration and the carbonation process in steel slag, revealing that the relationship is not always straightforward and depends on various factors, including slag type and reaction conditions.

2.4.4 Moisture Content and Relative Humidity

Ko, Chen, and Jiang (2015) introduced a novel aqueous carbonation technique employing a rotary kiln to expedite carbonation. This approach utilised a rotating kiln to mix CO_2, air, and gaseous water, thereby increasing the interaction area between CO_2 and EAF. Interestingly, the relative humidity (RH) played a significant role in influencing carbonation within the rotary kiln. The decline in pH value, illustrated in Figure 2.7, indicated a reduction in the carbonation reaction. It was found that carbonation consistently raised as the RH increased from 0 % to 60 %. However, when the RH reached 80 %, carbonation levels decreased. This phenomenon can be attributed to excessive moisture, which tends to block the surface pores of solids, thereby limiting the filtration of CO_2 to deeper layers.
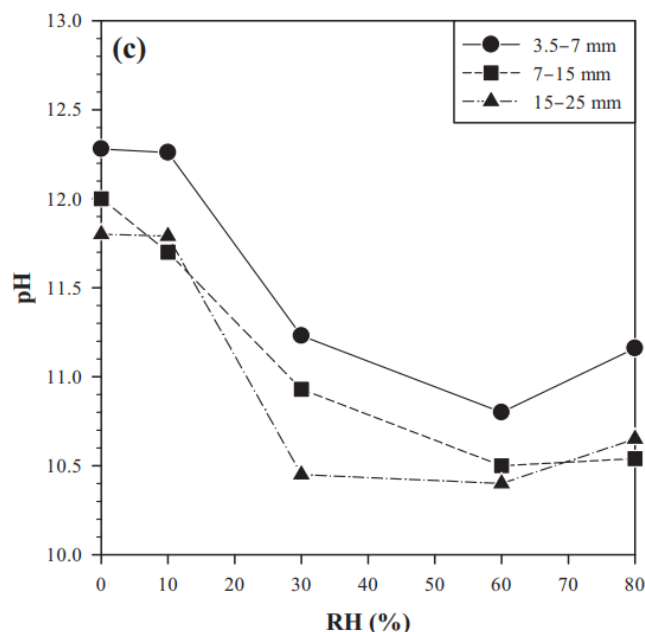
Figure 2.7: Effect of Relative Humidity (RH) on mineral carbonation (Ko, Chen, and Jiang, 2015)

The reduction in pH value, as depicted in Figure 2.7, served as a metric to gauge the progression of the mineralization reaction. Notably, carbonation efficiency gradually increased as the relative humidity (RH) escalated from 0 % to 60 %. However, a decline in carbonation was observed when the RH reached 80 %. This phenomenon can be ascribed to an abundance of moisture, which has a tendency to block the surface pores of solids, thus limiting the infiltration of CO_2 to deeper layers. Previous studies have underscored that a lower moisture concentration diminishes the dissolution of CO_2 and calcium ions. Conversely, an elevated moisture level leads to the obstruction of the pores within the steel slag, impeding the diffusion of CO_2. Both scenarios are incompatible with achieving rapid and effective carbonation. Consequently, determining ideal moisture content within the carbonation process is critical in ensuring efficiency and cost-effectiveness in carbonation procedures (Song, et al., 2021).

2.4.5 Particle Size

Despite the significant attention garnered by accelerated carbonation of industrial residues in recent years, a thorough and systematic evaluation of the influence of relevant operating parameters remains conspicuously absent from the scientific literature. While various factors are acknowledged to impact

carbonation reactions, encompassing both operational variables such as temperature, total pressure, partial CO_2 pressure, liquid-to-solid ratio, and pH, as well as solid material properties like particle size, porosity, surface area, and mineralogy, the relevance of particle size has been notably overlooked. Particle size represents a crucial, yet underappreciated characteristic of materials subjected to accelerated carbonation. Its influence on reaction kinetics, surface area available for CO_2 interaction, and overall carbonation efficiency warrants comprehensive exploration and consideration within the realm of carbonation research. Addressing this gap in understanding and acknowledging the significance of particle size in carbonation processes is essential for advancing the efficacy and sustainability of carbonation technologies in managing industrial residues and mitigating CO_2 emissions (Ramli, Kusin and Molahid, 2021).

In the study conducted by Polettini, Pomi, and Stramazzo (2016), the slag samples were separated into eight size classes using dry sieving. Each class was defined by specific cut sizes: 850 µm to 1,000 µm (C1), 500 µm to 850 µm (C2), 250 µm to 500 µm (C3), 150 µm to 250 µm (C4), 100 µm to 150 µm (C5), 63 µm to 100 µm (C6), 38 µm to 63 µm (C7), and <38 µm. Figure 2.8 illustrates the variation in CO_2 uptake, ranging by up to two orders of magnitude, from 0.47 % (C1) to 46.5 % (C6). This clearly indicates that the surface area of particles exposed to CO_2 significantly influences CO_2 uptake, surpassing the importance of elemental composition and mineralogy (Polettini, Pomi, & Stramazzo, 2016).
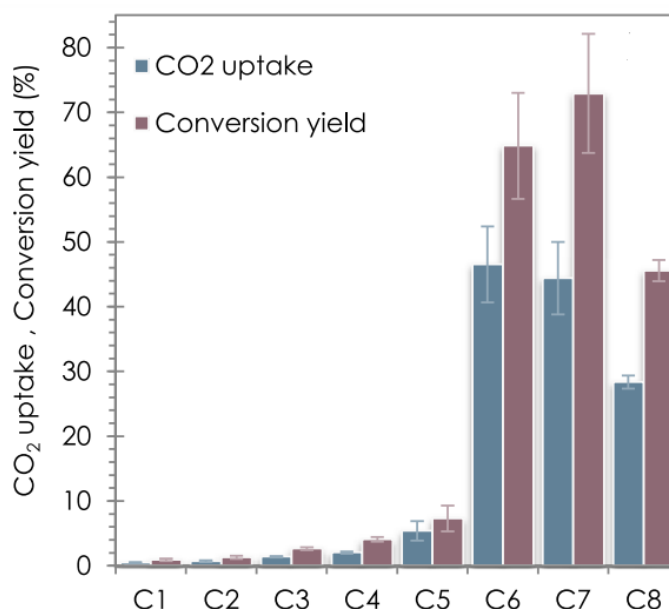
Figure 2.8: Carbonation Performance of the Eight Slag Classes (Polettini, Pomi and Stramazzo, 2016)

2.5   Suitable Feedstock

In the mineral carbonation process context, the ideal minerals for utilisation are oxides and hydroxides of alkaline-earth metals such as calcium (Ca) and magnesium (Mg). These minerals are favoured due to their rapid carbonation rates. Among them, Mg silicate is favoured over Ca silicate because of its abundance. Consequently, the mineral carbonation reaction involving Mg silicate can store a greater quantity of CO_2 than other carbonation reactions. Conversely, alkali metals like sodium (Na) and potassium (K) are not considered suitable for the carbonation process due to the instability of their corresponding carbonates, which readily dissolve in water. It is worth noting that oxides of Ca and Mg are not commonly used in the carbonation process because of their high reactivity and natural scarcity. Instead, the preference lies in silicate rocks that yield mineral oxides, typically used in industrial chemical plants for mineral carbonation reactions (Neeraj and Yadav, 2020).

Alkaline industrial residues can also serve as valuable sources of metal oxides for carbonation processes. Utilising accelerated carbonation with alkaline solid waste represents an effective and efficient method for capturing CO_2 from industrial flue gas emissions. Furthermore, these carbonated solid waste materials have the potential to be used as raw materials, partially replacing

clinker, or as aggregates in concrete, thereby reducing the reliance on Portland cement. This indirect outcome helps mitigate CO_2 emissions from the cement industry, contributing to efforts to combat global warming. Consequently, the mineralisation and utilisation of CO_2 through alkaline solid waste have garnered recognition as a promising technology that addresses both global warming and the challenges associated with alkaline solid waste treatment. Worldwide, examples of alkaline solid waste suitable for CO_2 mineralisation and utilisation include iron/steel slags, products from coal combustion, residues from fuel combustion, byproducts of mining and mineral processing, residues from incineration processes, waste from cement and concrete, and waste from pulp and paper mills (Chiang, et al., 2013).

The stabilization and reutilization of alkaline solid wastes hold special importance because these materials frequently contain elevated levels of calcium oxide and/or magnesium oxide, making them chemically unstable. When exposed to water and subjected to high pH conditions (typically exceeding 10), the active constituents within these waste materials can undergo hydration and react with CO_2 from flue gases. This reaction leads to the formation of carbonates through an accelerated carbonation process, which closely resembles natural weathering processes. Alternatively, the carbonated solid wastes can be repurposed as raw materials, either partially replacing clinker or serving as aggregates in concrete (Pan, et al., 2020).

2.6   Crystalline Polymorphs

Polymorphism refers to the phenomenon where a substance can crystallize into various crystal forms, each sharing the same chemical formula but featuring different arrangements of atoms or molecules within the crystal lattice (Carteret, et al., 2008). These polymorphs display distinct physical and chemical characteristics, including crystal morphology, stability, solubility, bioavailability, melting temperature, hygroscopicity, and chemical reactivity. These variations are pivotal in determining their suitability for diverse applications, carrying significant technical and financial implications across various fields. Indeed, the differences in crystalline structure play a crucial role in numerous industries such as pharmaceuticals, agrochemicals, pigments,

dyestuffs, foods, explosives, geophysics, energy storage, biominerals, and nonlinear and optical applications (Carteret, et al., 2008).

2.6.1 Calcium Carbonate

Calcium carbonate exhibits a diverse range of crystalline polymorphs under normal pressure conditions, including calcite, aragonite, and vaterite (Radha and Navrotsky, 2013). As noted in a recent study by Liendo, et al. (2022), calcium carbonate ($CaCO_3$) manifests in three distinct crystalline forms, ranked in terms of stability as calcite, aragonite, and vaterite. These crystalline phases of calcium carbonate feature differing crystal structures and morphologies, as depicted in Figure 2.9. Specifically, vaterite crystals possess a hexagonal structure, aragonite crystals display an orthorhombic structure, and calcite crystals exhibit a rhombohedral structure. The precipitation mechanism of $CaCO_3$ has undergone extensive investigation, revealing a process divided into three main stages:

(i) Initially, there is a predominant presence of Amorphous Calcium Carbonate (ACC) nucleation.

(ii) Subsequently, the unstable ACC dissolves and undergoes recrystallization into vaterite and calcite.

(iii) Finally, the metastable vaterite dissolves, leading to recrystallization into the most stable crystalline form, calcite.
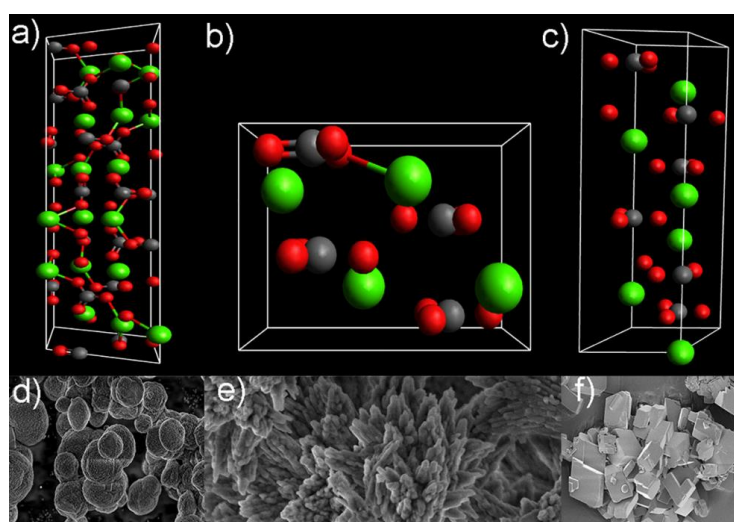
Figure 2.9: Crystal structures of $CaCO_3$ (Liendo, et al., 2022).

Nevertheless, alternative polymorphic forms like vaterite and aragonite can be induced by manipulating synthesis parameters, including temperature, pH, saturation levels, and concentrations of additives. For example, elevating temperatures beyond 40 °C and introducing Mg^{2+} ions at appropriate concentrations typically result in the production of metastable needle-like aragonite particles (Liendo, et al., 2022). Furthermore, studies have revealed that the synthesis of each polymorph is influenced by several factors, such as pH, temperature, concentration, the ratio of carbonate and calcium ions, the presence of additives, stirring, and reaction duration (Chang, et al., 2016). While temperature is often the primary determinant of $CaCO_3$ polymorphs during synthesis, other factors such as pH levels, ion concentrations, impurities, and the rate of CO_2 flow also interact in the processes of precipitation and crystallization. For instance, aragonite, typically formed at higher temperatures, may be obtained at lower temperatures in the presence of impurities like magnesium (Zhao, et al., 2013).

2.7 Stability of Carbonate Minerals

Carbonating magnesium and calcium silicates has emerged as an intriguing approach for the long-term storage of captured CO_2. However, to utilize mineral carbonation effectively in reducing atmospheric CO_2 emissions, even the slightest re-release or leakage of CO_2 cannot be tolerated, as it would diminish the total amount of captured and stored CO_2. Beyond contributing to atmospheric emissions, any CO_2 leakage from carbonate minerals utilized for CO_2 storage could also impact local environments. A sudden release of CO_2 gas could pose significant hazards, given its heavier-than-air properties, potentially leading to fatalities through asphyxiation. Even gradual leakage would have detrimental environmental effects, such as accumulation in soils or populated areas, with potentially dire consequences.

2.7.1 Stability in Water and Acid Rain Environments

Carbonate minerals exhibit limited solubility in water and do not decompose under normal conditions upon contact with it. For instance, when calcium carbonate dissolves in water, it dissociates into calcium ions (Ca^{2+}) and carbonate ions (CO_3^{2-}), without undergoing further decomposition. According

to the study (Teir, et al., 2006), the established thermodynamic stability of carbonates indicates that there should be no significant CO_2 leakage when exposed to water. However, they readily dissolve in strong acids, leading to the formation of mineral ions, carbon dioxide gas, and water. Consequently, there is a potential for CO_2 gas release upon the interaction of carbonate minerals with acidic precipitation, such as acid rain.

Ordinarily, rainfall possesses a slightly acidic nature with pH levels ranging from 5 to 7, owing to reactions with atmospheric CO_2, natural emissions of sulphur and nitrogen oxides, and specific organic acids. Human activities contribute to the continuous production of these acidifying compounds, resulting in the generation of sulfuric and nitric acid within rainwater. Despite the ability of acids to dissolve carbonate minerals, the quantity of sulphur and nitrogen oxides emitted is substantially lower compared to CO_2 emissions. The natural reserves of carbonate minerals are estimated to be around 90 million gigatons, underscoring the stability of carbonates. However, these natural deposits have formed over geological timescales, with the majority located underground. In contrast, manufactured magnesium and calcium carbonates are produced within hours or less, likely through precipitation, resulting in a powdered form. Due to their smaller particle size, these manufactured carbonates are more readily soluble than large blocks of natural carbonate minerals. Consequently, acid rain may potentially induce localized CO_2 releases from carbonate mineral storage sites (Teir, et al., 2006).

2.7.2   Thermal Stability

The thermal stability of carbonate mineral plays a critical role in its effectiveness for carbon capture, primarily determined by the decomposition temperatures of its key constituents, calcium carbonate and magnesium carbonate. Notably, the main components of slag are calcium oxide and magnesium oxide, resulting in carbonated slags containing elevated levels of $CaCO_3$ and $MgCO_3$. Consequently, during carbonation processes, these compounds act as potent CO_2 absorbers, underscoring the pivotal significance of their thermal stability in facilitating carbon capture endeavours.

Historically, certain carbonates have been observed to decompose upon heating, as evidenced by ancient practices such as the production of lime

from limestone (calcium carbonate), and more contemporary applications like furnace-linings made from dolomite and magnesite, which are polymorphs of magnesium carbonate (Wells, 1934). Moreover, recent studies, such as that conducted by Karunadasa, et al. (2019), shed light on the thermal decomposition behaviour of calcite, a calcium carbonate polymorph. This research reveals that calcite begins to decompose slowly around 700 °C, with rapid decomposition occurring beyond 750 °C. Similarly, investigations into magnesite, another polymorph of $MgCO_3$, indicate a sluggish decomposition rate below 560 °C, followed by a gradual increase starting at 580°C and peaking at 600 °C (Wells, 1934).

2.8   Analytical Method

2.8.1   Scanning Electron Microscopy (SEM) Analysis

Scanning Electron Microscopy (SEM) has emerged as an indispensable tool across numerous scientific domains, offering unparalleled insights into the microscopic world with its high-resolution imaging capabilities. Unlike traditional microscopy techniques, SEM operates on the principle of electron emission, enabling the examination of materials at nanometre to micrometre scales. SEM's superiority lies in its ability to produce highly detailed grayscale images, facilitating precise analysis of both organic and inorganic materials. With magnification capabilities reaching up to 300,000x and even beyond in modern models, SEM offers a profound understanding of material morphology, surface topography, and elemental composition. Moreover, SEM is often coupled with Energy Dispersive X-ray spectroscopy (EDX), augmenting its analytical capabilities by providing qualitative and semi-quantitative elemental analysis (Mohammed and Abdullah, 2018).

According to Nielsen, et al. (2020), scanning electron microscopy (SEM) can be utilized to study the microstructure of electric arc furnace (EAF) slags before and after carbonation. This enables observation of the changes in morphology and distribution of mineral phases within the slag particles. Furthermore, SEM offers detailed insights into the surface topography and texture of EAF slag particles, which are crucial for understanding the reactivity of the slag surface with carbon dioxide during the carbonation process.

Furthermore, in the research by Nicol (1975), the application of scanning electron microscopy (SEM) represents a transformative approach to delving into the micro and nanoscale intricacies of materials, offering insights beyond the capabilities of traditional light microscopy. The SEM analysis process is as follows:

(i) SEM analysis commences with the emission of a high-energy electron beam, typically ranging between 100 and 30,000 electron volts, facilitated by a thermal source.

(ii) To achieve precise imaging, SEM employs lenses to compress the initially broad electron beam spot, directing focused electrons onto the specimen. This process results in spot sizes typically smaller than 10 nm, with electrons penetrating to a depth of 1 μm, generating signals for image formation.

(iii) Image acquisition proceeds point by point as the electron beam scans discrete locations in straight lines, guided by scan coils until a rectangular raster is formed on the specimen's surface. The adjustments in magnification control the area covered by the scan coils. Modern SEMs incorporate automatic adjustments to accommodate variations in working distance, ensuring optimized magnification.

(iv) Electron detectors play a crucial role in capturing emitted signals from the scanned sample, essential for image generation. Both secondary electrons (SE) and backscattered electrons (BSE) contribute to image formation. Various types of detectors, including scintillator detectors, enable the detection of these signals.

(v) The acquired signals are displayed on the viewing screen, allowing operators to fine-tune brightness and intensity to obtain clear images. For finer details, magnifications exceeding 10,000x are often employed.

(vi) The choice of electron voltage mode significantly influences image details. Low accelerating voltages (<5 kV) yield surface-rich images, while higher voltages (15 kV to 30 kV) penetrate deeper into the sample, revealing internal structures.

(vii)   SEM images offer a partly three-dimensional perspective, primarily visualizing sample topography in terms of shape, size, and surface texture. The abundance of BSE and SE signals is influenced by the angle of inclination of the sample surface, with steeper angles enhancing signal intensity and topographic contrast.

2.8.2   Energy Dispersive X-Ray Spectroscopy (EDX) Analysis

Energy Dispersive X-ray Spectroscopy (EDX, also known as EDS or EDXS) is a fundamental analytical technique extensively utilized in materials science and allied disciplines for the elemental analysis and compositional characterization of solid samples. EDX operates on the fundamental principle of X-ray fluorescence, where high-energy electrons, typically generated by an electron beam in a scanning electron microscope (SEM), interact with the atoms in a sample, leading to the emission of characteristic X-rays. These X-rays are specific to the elements present in the sample, and their energy levels correspond to the atomic structure of the emitting elements. The application of EDS involves directing an electron beam onto the sample surface, resulting in interactions that produce characteristic X-rays. These X-rays are then detected by an energy-dispersive spectrometer, which sorts and quantifies them based on their energy levels. By analysing the energy spectrum of the emitted X-rays, researchers can identify the elements present in the sample and determine their relative concentrations. This information is crucial for understanding the composition, structure, and properties of materials.

According to Hodoroaba (2020), there are significant advantages of EDX include its capability for non-destructive elemental analysis of samples, high sensitivity even at low concentrations, and the ability to analyse a wide range of elements from the entire periodic table. Additionally, EDX is relatively fast and can provide spatially resolved elemental information, making it valuable for mapping elemental distributions within samples. However, EDS also has some limitations. Despite its capability to detect a wide range of elements, such as those present in the periodic table, it faces challenges in detecting light elements like hydrogen and helium due to their minimal X-ray emissions. Moreover, distinguishing between elements with similar atomic

numbers, such as carbon and nitrogen, poses difficulties for the technique. Additionally, ensuring accurate results requires meticulous sample preparation, and EDX may encounter issues such as X-ray fluorescence from substrate materials or detector dead-time effects, which can affect the precision of quantitative analysis. These factors should be carefully considered when utilizing EDX for materials analysis (Shindo and Oikawa, 2002).

2.8.3   X-Ray Diffraction (XRD) Analysis

X-ray Diffraction (XRD) analysis is a powerful analytical technique employed to ascertain the crystal structure of materials through the analysis of the diffraction pattern generated upon X-ray interaction with a sample. This interaction results from the incidence of X-rays on atoms within a crystal lattice, causing scattering in various directions. The ensuing diffraction pattern yields insights into the arrangement of atoms within the crystal lattice, enabling researchers to discern the crystal structure and phases within the sample. Crystalline structures exhibit a systematic and periodic arrangement of atoms or ions in a three-dimensional array. Within crystals, atoms are regularly spaced, forming planes that are separated by a consistent distance. These interplane distances are distinctive characteristics of each crystalline species. X-rays, on the other hand, are composed of electrostatic and electromagnetic fields oscillating in periodic cycles perpendicular to one another and to their direction of propagation through space. With wavelengths typically ranging from 10^{-3} nanometres to 10^{1} nanometres, X-rays are generated within an evacuated X-ray tube through the bombardment of a metal target (anode) by high-velocity electrons (Whittig and Allardice, 2018).

According to Bunaciu, Udriştioiu, and Aboul-Enein (2015), the applications of X-ray diffraction (XRD) are extensive, spanning a diverse array of fields including materials science, geology, chemistry, pharmacy, and biology. XRD serves various purposes, encompassing phase identification, crystal structure determination, quantitative analysis of crystalline phases, texture analysis, and investigation of structural alterations induced by external stimuli such as temperature or pressure. The advantages of XRD are manifold. It boasts a non-destructive nature, high sensitivity to crystalline materials, and the capacity to provide detailed structural information about samples. Moreover,

XRD exhibits versatility, capable of analysing an array of materials ranging from powders and thin films to bulk solids and nanomaterials. However, XRD is not without its limitations. It necessitates samples to be in crystalline form, thereby constraining its applicability exclusively to crystalline materials. Amorphous or non-crystalline samples cannot undergo analysis via XRD. Additionally, the preparatory process for samples can be time-intensive, and proficient interpretation of data may require specialized equipment and expertise.

2.8.4 Thermogravimetric Analysis (TGA)

Thermogravimetric Analysis (TGA) belongs to the field of thermal analysis, which investigates how the weight of a substance changes over time or with temperature variations. This technique involves recording the weight change profile of a sample as it undergoes controlled heating or cooling. The fundamental principle of TGA lies in its ability to study the mass change of a sample under controlled conditions. Consequently, TGA is commonly employed to examine various thermal phenomena such as absorption, adsorption, desorption, vaporization, sublimation, decomposition, oxidation, and reduction. Moreover, TGA can be utilized to assess the volatile or gaseous products released during these chemical processes, particularly in samples such as nanomaterials, polymers, polymer nanocomposites, fibres, paints, coatings, and films. Beyond evaluating the thermal stability of samples, TGA enables the investigation of reaction kinetics under different conditions (Loganathan, et al., 2017). One of its primary applications lies in assessing the thermal stability of materials. By tracking the weight change of a sample as it undergoes controlled heating or cooling, TGA enables researchers to identify temperatures at which materials undergo decomposition, vaporization, or other thermal events. This information is crucial in industries such as materials science, pharmaceuticals, and food processing, where understanding thermal stability is essential for product development and quality control (Loganathan, et al., 2017).

2.9   Summary

Chapter 2 offers a comprehensive literature review on mineral carbonation for CO_2 conversion, emphasizing the role of temperature in optimizing efficiency and stability. It covers direct and indirect mineralization methods, detailing their efficiency in CO_2 sequestration. The reaction mechanisms are analysed, highlighting temperature's influence on thermodynamics and kinetics. Key factors like temperature, pressure, CO_2 concentration, and particle size are identified as crucial for enhancing carbonation efficiency. The suitability of feedstocks, especially natural minerals and industrial by-products such as Electric Arc Furnace (EAF) slag, is discussed in terms of reactivity and availability. The formation of crystalline polymorphs like vaterite and calcite and their stability under different conditions are examined. Thermal stability studies review the resilience of carbonate minerals to thermal cycling, essential for long-term CO_2 storage. Analytical methods such as Energy-Dispersive X-ray Spectroscopy (EDX), Scanning Electron Microscopy (SEM), X-ray Diffraction Analysis (XRD), and Thermogravimetric Analysis (TGA) are explained for their roles in characterizing the mineralization process and assessing CO_2 conversion efficiency. Overall, Chapter 2 underscores temperature's significant impact on enhancing the mineralization process, providing a foundation for the current study's experimental design and objectives.

CHAPTER 3

METHODOLOGY AND WORK PLAN

3.1   Introduction

This section offers an introductory overview of the experimental methodology employed in optimizing temperature parameters to enhance the mineralization process. The primary goal of this study is to maximise the efficiency of CO_2 conversion and assess the stability of the formed carbonate minerals.

Figure 3.1 illustrates the methodology outlined in this chapter, which encompasses a series of meticulously planned steps, beginning with the preparation of raw materials, pre-treatment of electric arc furnace (EAF) slags, and concluding with the carbonation process. Following the carbonation process, the subsequent phase involves conducting laboratory tests to analyse the properties of the formed carbonate minerals. After the mineralization process is completed, the carbonate minerals formed will undergo several laboratory tests to assess their characteristics. These tests include scanning electron microscopy (SEM), energy dispersive X-ray spectroscopy (EDX), X-ray diffraction (XRD) analysis, and thermogravimetric analysis (TGA). Each of these tests provides valuable insights into the morphology, elemental composition, crystalline structure, and thermal behaviour of the carbonate minerals formed during the carbonation process.
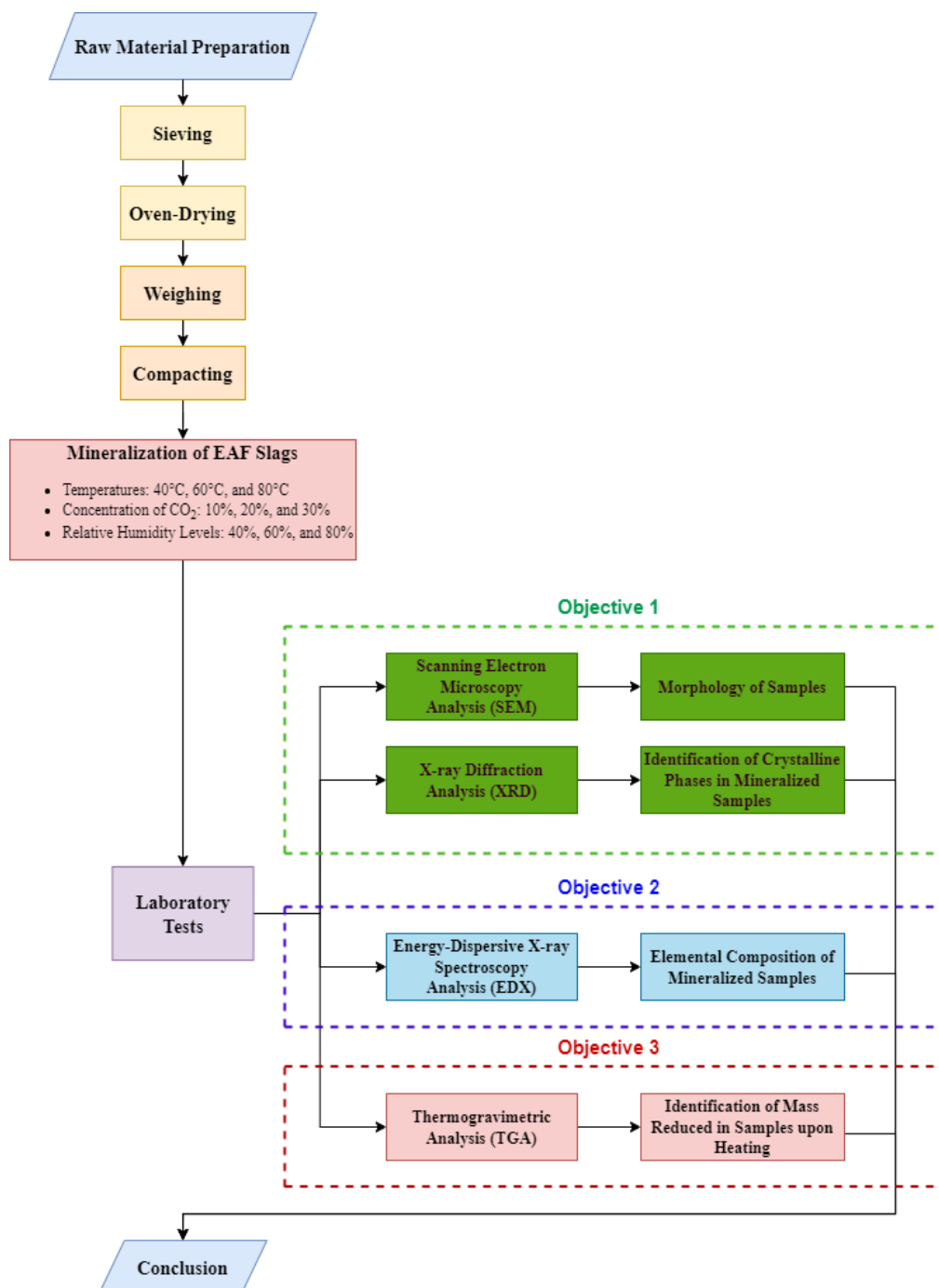
Figure 3.1: Methodology Flowchart.

3.2   Raw Materials Preparation

In this study, electric arc furnace (EAF) slags originating from Penang state, Malaysia, were selected as the sample material for the mineralization experiment due to their relevance to the local context and availability. Figure 3.2 illustrates that EAF slags have a dark, metallic appearance, attributed to the presence of iron oxides and other metal compounds. Additionally, the texture of EAF slags ranges from coarse to fine, with coarse particles exhibiting a rough, irregular texture, while finer particles may feel smoother to the touch. Several steps are undertaken to prepare the EAF slags for the subsequent mineralization process. These steps are crucial to ensure the accuracy and reliability of the experimental results.

Figure 3.2: Electric Arc Furnace (EAF) Slags.

3.2.1   Oven-Drying

The first step involves oven-drying the EAF slags to remove moisture. As EAF slags are porous, they may retain moisture, potentially influencing the experimental outcomes. Therefore, by subjecting the slags, contained within trays as depicted in Figure 3.3, to an oven set at 100 °C for a duration of 24 hours, any hidden moisture is eliminated, thereby maintaining the integrity of the experimental conditions.

Figure 3.3: Oven-Drying of EAF Slags.

3.2.2 Sieving

As previously noted, variations in the particle sizes of EAF slags could impact their efficiency in CO_2 conversion. Therefore, it was necessary to separate the slags into coarse and fine particles to ensure consistency in the experimental setup. In this study, a specific particle size range of 0.8 mm to 2.36 mm was chosen to maintain uniformity. A sieve stack containing screens with different mesh sizes, as depicted in Figure 3.4, was employed to achieve this. Additionally, a sieve shaker was utilized to aid in the separation of particles based on their size. These tools worked together to ensure that the desired particle size range was attained, thereby improving the reliability and accuracy of the subsequent mineralization experiments.

Figure 3.4: Sieve Stack.

3.3 Pre-Treatment of EAF Slags

In this study, the EAF slags underwent a crucial pre-treatment stage prior to the mineralization process. This pre-treatment involves compacting the EAF slags into cylindrical shapes with specific dimensions: a diameter of 20 mm and a height of 10 mm, as visually depicted in Figure 3.5.

Figure 3.5: Compacted EAF Slag Sample.

The process began with the measurement of 10.00 g of oven dried EAF slags using a weighing balance. To account for potential weight reduction of the

EAF slags during demoulding or movement of samples after the compaction process, an additional 0.50 g of EAF slags was added before compaction. This ensured that the weight of each sample remained around 10.00 g. Figure 3.6 illustrates the weight of a 10.00 g sample decreasing after experienced some movement following the compaction process.

Figure 3.6: Variation in Sample Weight after Post-Compaction Movement.

These slags were then carefully placed into a stainless-steel mould designed to shape them into cylinders. Subsequently, the manually operated hydraulic compaction machine applied a pressure of 20 MPa to compact the slags within the mould thoroughly. Following compaction, the formed samples were demoulded, ensuring their structural integrity and adherence to the specified dimensions. All compacted samples were promptly transferred and stored in an oven to prevent potential moisture absorption. This step was essential to maintain the dryness of the samples, eliminating any moisture that could affect the subsequent carbonation process. The EAF slags were prepared optimally for the ensuing mineralization experiments by meticulously following these pre-treatment procedures. This meticulous attention to detail ensured the integrity and reliability of the experimental setup, ultimately contributing to the accurate assessment of CO_2 conversion efficiency and stability of formed

carbonate minerals. Figure 3.7 displays the stainless-steel mould used in this study, while Figure 3.8 depicts the hydraulic compaction machine utilized.

Figure 3.7: Stainless Steel Mould with 20mm Diameter.

Figure 3.8: Hydraulic Compaction Machine.

3.4   Mineralization of EAF Slags

In this study, the mineralization process of EAF slag samples was conducted under diverse temperature conditions, ranging from 40 °C to 80 °C with 20 °C intervals. Additionally, two other manipulating parameters: the concentration of CO_2 and relative humidity levels, were varied to simulate different reality conditions and determine optimised temperature parameters under these conditions. The CO_2 concentration varied from 10 % to 30 % with 10 % intervals, while relative humidity levels range from 40 % to 80 % with 20 % intervals. The maximum CO_2 gas concentration and temperature in the carbonation chamber were 30% and 99.9°C, respectively, as restricted by equipment capabilities.

Following the previous procedure, compacted EAF slag samples were placed into the carbonation chamber for the mineralization process, as depicted in Figure 3.9. The EAF slag samples underwent mineralization for a duration of 24 hours. A total of 27 sets of samples were carbonated under different temperatures and simulated conditions by the end of the experiment. Once the 24 hours were up, the carbonated samples were immediately sent for laboratory tests.

Figure 3.9: Carbonation Chamber.

3.5   Laboratory Tests

In this section, four laboratory tests were conducted to determine the characteristics or properties of the carbonated EAF slags. These tests were crucial for data analysis to identify the effects of different temperature on the mineralization process, maximized CO_2 conversion efficiency under different conditions and the stability of the formed carbonate mineral.

3.5.1   Scanning Electron Microscopy (SEM) Analysis

Scanning electron microscopy (SEM) is a powerful imaging technique used to examine the surface morphology and microstructure of materials at high magnification. By scanning a focused beam of electrons across the sample surface, SEM produces detailed images with high resolution, allowing for the visualization of features at the nanoscale level. SEM is particularly useful for characterizing the surface topography, particle size, shape, and distribution of materials. Additionally, SEM could be coupled with energy-dispersive X-ray spectroscopy (EDX) to provide elemental analysis of the sample, further enhancing its capabilities. Figure 3.10 shows the scanning electron microscope utilized in the research.

Figure 3.10: Scanning Electron Microscope.

To prepare the carbonate EAF slag sample for SEM analysis, the sample was first crushed and ground into fine particles using a mortar and pestle. Then, carbon tape was applied onto SEM specimen stubs to serve as an adhesive. The ground sample was carefully transferred onto the carbon tape, ensuring even distribution and complete coverage. Gentle pressure was applied to remove any air bubbles or gaps. Figure 3.11 illustrates the specimen stubs and mounts used in the SEM.

Figure 3.11: SEM Specimen Stubs and Mounts.

Once mounted and labelled, the sample was inserted into the SEM chamber, imaging parameters such as brightness, contrast, and magnification were adjusted to capture high-resolution images of the sample surface, revealing its morphology and microstructure. In this research, the magnification scale of the SEM images of the sample surfaces was set to 1,000 x. Figure 3.12 shows the high-resolution image of the uncarbonated sample surface under SEM.
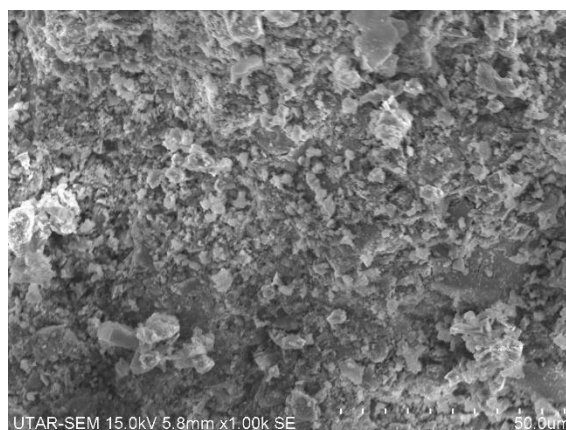
Figure 3.12: SEM Image of EAF Slag Sample.

3.5.2 Energy Dispersive X-ray Spectroscopy (EDX) Analysis

Energy-Dispersive X-ray Spectroscopy (EDX) is a technique utilised to determine the elemental composition of materials. When a sample is bombarded with high-energy electrons in an SEM or an EDX instrument, it emits characteristic X-rays that are characteristic of the elements present. EDX detects and analyses these X-rays to provide qualitative and quantitative information about the elemental composition of the sample. It offers rapid elemental analysis with high sensitivity and specificity, making it suitable for a wide range of materials and applications. EDX spectra provide information on elemental peaks and their intensities, enabling the identification and quantification of elements in the sample. Given that EDX is commonly coupled with scanning electron microscopy (SEM), the preparation of samples for EDX analysis can be executed simultaneously with SEM analysis. Consequently, once the sample is mounted on the SEM specimen stub and carbon tape, it can undergo direct analysis employing both SEM and EDX without necessitating additional sample preparation steps.

3.5.3 X-ray Diffraction (XRD) Analysis

X-ray Diffraction (XRD) is a technique used to analyse the crystalline structure and phase composition of materials. By measuring the diffraction patterns produced when X-rays interact with the crystal lattice of a sample, XRD enables the identification of crystalline phases and determination of crystallographic parameters. XRD is non-destructive and highly sensitive to the arrangement of atoms in the material, allowing for the detection of even minor crystalline phases.

It provides information about crystal symmetry, lattice parameters, and crystal size, making it valuable for phase identification and structural analysis in materials science, geology, and chemistry. Figure 3.13 depicts the X-ray Diffractor utilized in this study.

Figure 3.13: X-Ray Diffractometer (XRD).

In the procedure for preparing samples for X-ray Diffraction (XRD) analysis, the first step involved further grinding the small particles of carbonated EAF slag samples until they reached a powdered form. Once the sample was finely powdered, it was filled into the concave on the sample specimen holder, as shown in Figure 3.14. Subsequently, manual compression was applied using a piece of glass to ensure that the sample was tightly compacted within the concave. This compression was crucial to prevent the sample from falling out during scanning in the XRD machine. During the scan, the sample was rotated from a specific angle to another, depending on the scanning range determined for the analysis. In this study, the scanning range spanned from 5 ° to 85 ° and the entire XRD analysis was expected to take approximately 40 minutes to complete.
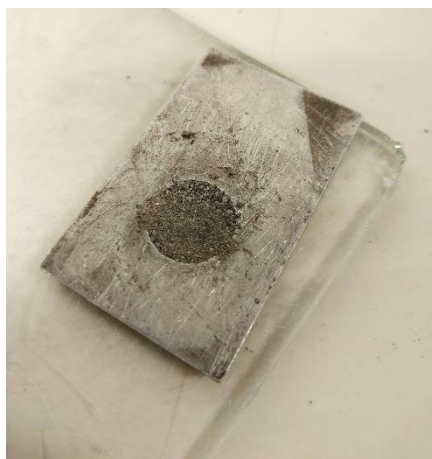
Figure 3.14: XRD Sample Specimen Holder.

The XRD analysis in this study adhered to a configured setup utilizing a gonio scan axis equipped with specific parameters to ensure precise data collection. The scan range spanned from 5.0000° to 85.0000° 2θ, with a fine step size of 0.0200° 2θ, while maintaining a scan step time of 1.0000 seconds and a 0.0000° 2θ offset for alignment accuracy. Additionally, consistency in data acquisition across samples was ensured through the utilization of a pre-set time scan type. Control over beam divergence during measurements was achieved by employing a fixed divergence slit type with a size of 1.0000°. To optimize the detection of diffracted X-rays, the sample length was limited to 10.00 mm, with a receiving slit size of 0.1000 mm. Experiment reproducibility was guaranteed by operating at a stable measurement temperature of 25.00 °C. Moreover, the XRD system utilized a Cu anode material with characteristic wavelengths of K-Alpha1 at 1.54060 Å and K-Alpha2 at 1.54443 Å, which was essential for accurate data analysis.

3.5.4   Thermogravimetric Analysis (TGA)

Thermogravimetric Analysis (TGA) is a technique used to study the thermal properties and decomposition behaviour of materials as a function of temperature. TGA provides information about weight loss events such as dehydration, decomposition, and oxidation by measuring the change in sample mass with temperature. TGA offers precise control over heating rates and temperature conditions, allowing for detailed analysis of thermal behaviour. It was versatile and can be used to investigate various thermal processes, including

decomposition kinetics, phase transitions, and stability. TGA data could be used to determine the composition, purity, and thermal stability of materials. Figure 3.15 shows the Thermogravimetric Analyzer used in this study.

Figure 3.15: Thermogravimetric Analyzer.

During the thermal analysis of the carbonated samples, specific conditions were set to facilitate accurate measurement of the sample's thermal properties. The analysis was conducted under a nitrogen (N_2) atmosphere, with a continuous flow rate of 50 ml/min. Additionally, a purge gas was employed at a flow rate of 20 ml/min to maintain a stable environment within the TGA instrument. The heating rate is set to 10 °C/min, ensuring a gradual increase in temperature over time. The temperature range spanned from 25 °C to 900 °C, covering a broad spectrum to capture any changes in sample mass throughout the heating process. These controlled conditions enabled precise characterization of the thermal behaviour and decomposition kinetics of the samples during TGA analysis.

3.6   Summary

The targeted products of the carbon mineralization process in this study were calcium carbonate and magnesium carbonate, as these two alkaline metals constituted a higher proportion of the EAF slags. Before the mineralization process, 10.00 g of EAF slags were underwent mechanical pre-treatment, being compacted them into cylinders with a diameter of 20 mm and a height of 10 mm using a hydraulic compaction machine. Subsequently, the pre-treated slag samples were placed in the carbonation chamber for 24 hours to undergo mineralization process. In this research, the mineralization process of EAF slags was conducted under three different temperature parameters: 40 °C, 60 °C, and 80 °C. Additionally, the mineralization processes with different temperature parameters were carried out under various simulated conditions, which included different concentrations of CO_2 gases (10 %, 20 %, and 30 %) and humidity levels (40 %, 60 %, and 80 %). This comprehensive approach ensured that the effects of temperature on the mineralization process remained consistent across a range of conditions. This resulted in a total of 27 sets of carbonated samples, which subsequently underwent several laboratory tests to analyse and determine the carbon conversion efficiency and stability of the carbonate minerals formed. These laboratory tests included SEM, EDX, XRD, and TGA analysis.

CHAPTER 4

RESULTS AND DISCUSSION

4.1   Introduction

This chapter describes the outcomes and explanations of four laboratory tests conducted to evaluate and determine the effects of different temperatures on the mineralization process, the maximised CO_2 conversion efficiency of the mineralization process under different conditions, and the thermal stability of the formed carbonate minerals.

In this research, Scanning Electron Microscopy (SEM) is utilised to study the morphology and microstructure of electric arc furnace (EAF) slags before and after the mineralization process. The test outcomes determine the changes in the microstructure of the samples by identifying any presence of specific crystal structures, which indicate the formation of carbonate minerals in the samples.

In this research, Energy-Dispersive X-ray spectroscopy (EDX) analysis serves as a fundamental tool for determining the elemental composition of the samples. Additionally, by detecting and quantifying the elemental composition of the slags before and after mineralization, the test outcomes provide insight into the changes in the elemental composition of carbon, expressed as a percentage by weight.

In addition, X-ray diffraction (XRD) analysis plays a critical role in identifying the precise crystal structures and mineral phases present in both the initial EAF slags and the products of the mineralization process. Additionally, XRD provides valuable information regarding the mineral products purity, crystallinity, and phase composition.

Thermogravimetric analysis (TGA) serves as a technique for investigating the thermal stability of the carbonate minerals formed during the mineralization process. The test outcomes provide insight into the characterization of decomposition processes, phase transitions, and thermal stability by subjecting samples to controlled temperature variations and monitoring changes in weight.

4.2　　Energy-Dispersive X-Ray Spectroscopy (EDX)

In this research, EDX was employed to analyse the elemental composition of electric arc furnace (EAF) slags both before and after mineralization. The aim was to determine the CO_2 conversion efficiency of the mineralization process under various temperature parameters and simulated conditions. EAF slags are predominantly comprised of metal oxides, which react with CO_2 to form carbonate minerals. Table 4.1 illustrates the elemental composition of EAF slags, reported as weight percentages, prior to mineralization, with particle sizes ranging from 0.8 mm to 2.36 mm. It reveals the presence of oxygen, calcium, magnesium, aluminium, and silicon, with mean weight percentages of 16.27 %, 62.72 %, 2.63 %, 4.82 %, and 13.20 %, respectively. Additionally, no carbon element was found within the sample before mineralization.

Table 4.1:　Elemental Composition of EAF Slags with Particle Sizes Ranging from 0.8 mm to 2.36 mm.

Element	Sample			Mean
	1	2	3	
	(wt%)	(wt%)	(wt%)	(wt%)
O	16.35	16.49	15.98	16.27
Ca	64.13	60.85	63.17	62.72
Mg	2.20	3.42	2.28	2.63
Al	3.85	4.56	6.06	4.82
Si	13.58	13.54	12.48	13.20

Notably, calcium, magnesium, and aluminium are present as metal oxides, whereas silicon exists as silicon dioxide (SiO_2), a metalloid. Calcium emerges as the most abundant element in the EAF slags. Magnesium exhibits higher reactivity than calcium, but its abundance is only 2.63 %. Conversely, silicon ranks second in abundance at 13.20 %, yet its reactivity with CO_2 is lower than that of calcium. According to a study by Yong, Tse, and Chen (2018), chemical reactions between SiO_2 and CO_2 were observed only at 26 GPa and 726.85 °C. Therefore, despite its higher abundance, silicon is unlikely to react significantly with CO_2 to form silicon carbonate. Given the abundance and reactivity of calcium in the sample, the predominant mineralization product is expected to be calcium carbonate.

The CO_2 conversion efficiency of the mineralization process can be determined by measuring the changes in the carbon content of the EAF slag samples before and after the mineralization process. These changes in carbon element content result from the chemical reaction between calcium oxide and CO_2, producing calcium carbonate. Table 4.2 demonstrates the elemental composition of carbon within the carbonated EAF slag samples under different temperature parameters and various simulated conditions, including different concentrations of CO_2 gases and relative humidity levels.

Table 4.2:   Elemental Composition of Carbon in the Carbonated EAF Slag Samples

Simulated Condition	Sample No	Temperature (°C)	Concentration of CO_2 (%)	Humidity Levels (%)	Elemental Composition of Carbon (wt%)
1	1	40	10	40	0.36
	2	60			0.97
	3	80			2.48
2	4	40	20	40	0.99
	5	60			1.89
	6	80			3.02
3	7	40	30	40	1.46
	8	60			2.56
	9	80			3.55
4	10	40	10	60	1.55
	11	60			2.64
	12	80			4.61
5	13	40	20	60	3.19
	14	60			4.71
	15	80			6.44
6	16	40	30	60	4.22
	17	60			6.11
	18	80			8.31

Table 4.2 (Continued)

	19	40			3.26
7	20	60	10	80	5.46
	21	80			7.53
	22	40			5.16
8	23	60	20	80	7.32
	24	80			9.70
	25	40			6.84
9	26	60	30	80	9.31
	27	80			12.79

The tabulated data has been further plotted into three graphs representing the carbon element content (wt%) versus temperature (°C) for better analysis, as depicted in Figures 4.1 to 4.3, respectively. Figure 4.1 demonstrates the relationship between carbon element content and temperature under simulated conditions 1, 2, and 3. The increasing trend in carbon content is evident across all three simulated conditions as temperature rises. For instance, the carbon element content at a common temperature parameter of 80 °C for these three conditions is 2.48 %, 3.02 %, and 3.55 %, respectively. This observation suggests that higher temperatures enhance CO_2 conversion efficiency in the mineralization process, despite variations in CO_2 gas concentrations.

Figure 4.1: Graph of Carbon Element Content versus Temperature under Simulated Conditions 1, 2, and 3 at Relative Humidity of 40%.

Furthermore, it is observed from Figure 4.1 that the carbon content tends to be higher at higher CO_2 concentrations, even when the temperature and humidity levels are consistent across simulated conditions 1, 2, and 3. This suggests a significant influence of CO_2 concentration on carbon content. In addition, Figure 4.2 presents the graph depicting the carbon element content

(wt%) versus temperature (°C) for simulated conditions 4, 5, and 6. Like the results observed in conditions 1, 2, and 3, the carbon element content in conditions 4, 5, and 6 increases as temperature rises, despite varying CO_2 concentrations. It is worth noting that the overall carbon element content in conditions 4, 5, and 6 is higher compared to conditions 1, 2, and 3. This suggests an influence of humidity levels on the mineralization process.
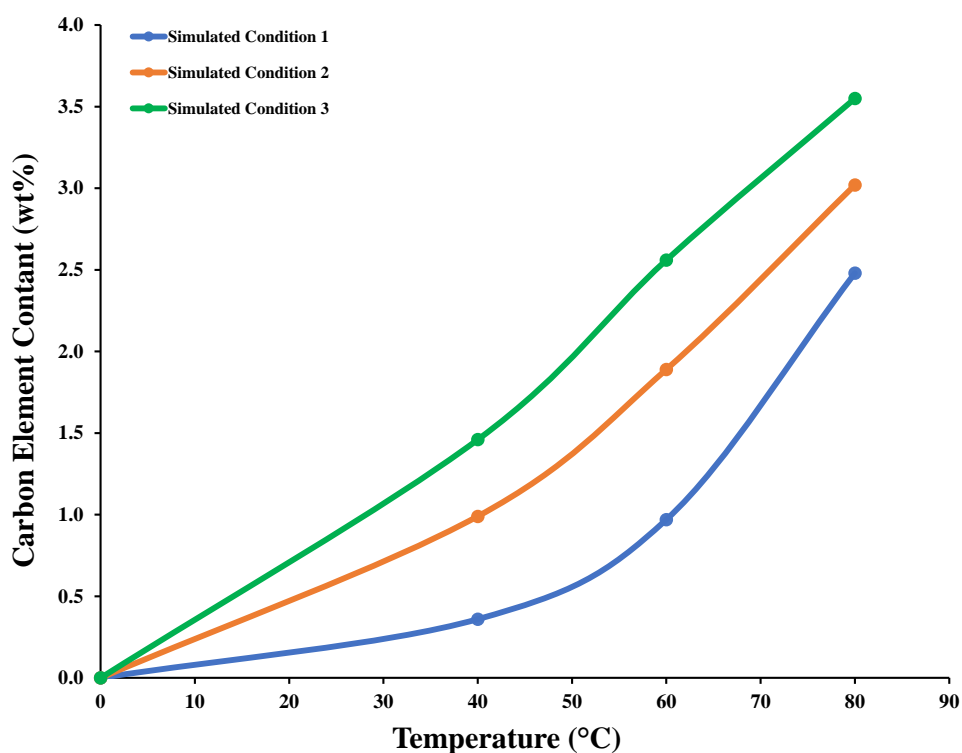

Figure 4.2: Graph of Carbon Element Content versus Temperature under
Simulated Conditions 4, 5, and 6 at Relative Humidity of 60%.

The graph of carbon element content versus temperature for simulated conditions 7, 8, and 9 is shown in Figure 4.3. It demonstrates a steady rise in carbon content as temperatures increase across all three conditions, despite different CO_2 concentrations, indicating that the higher temperatures lead to better carbonation efficiency of the mineralization process. Since no carbon element is found in the samples before mineralization, the CO_2 conversion efficiency can be defined as the increase in the carbon element content within the samples after mineralization. The CO_2 conversion efficiency at a temperature of 80 °C is found to be the highest compared to that at 40 °C and 60 °C across all nine simulated conditions. Additionally, significant influences

of rising humidity levels on improving the carbonation efficiency of the mineralization process are observed when temperature parameters and CO_2 concentrations are considered. For example, when the temperature and CO_2 concentration remain at 80 °C and 30 %, the CO_2 conversion efficiency of mineralization at humidity levels of 40 %, 60 %, and 80 % is 3.55 %, 8.31 %, and 12.79 %, respectively.
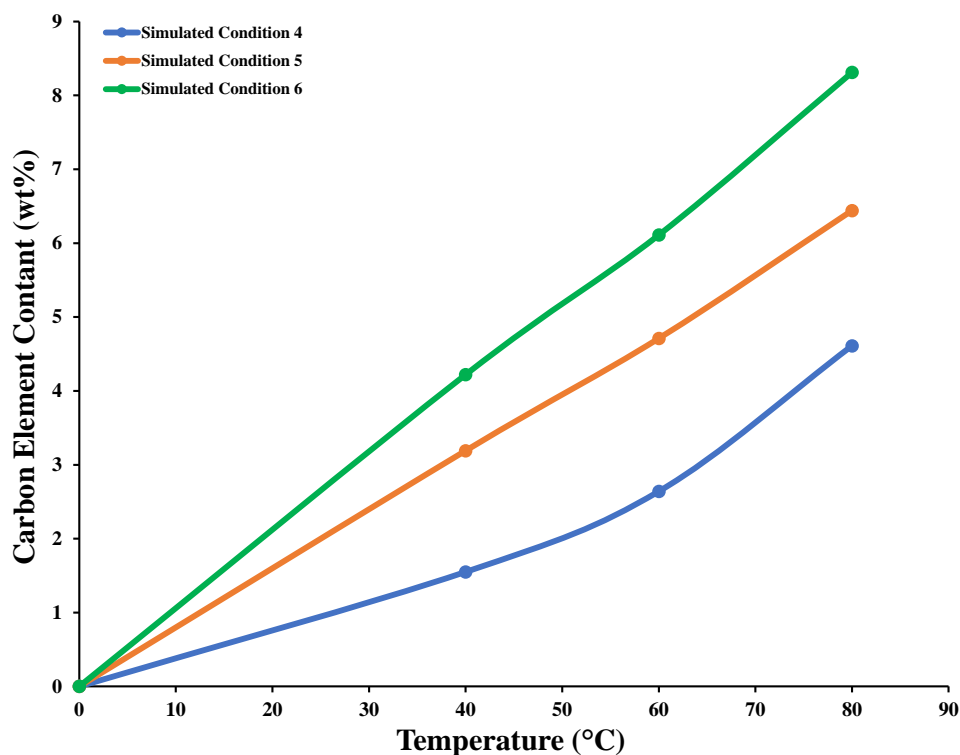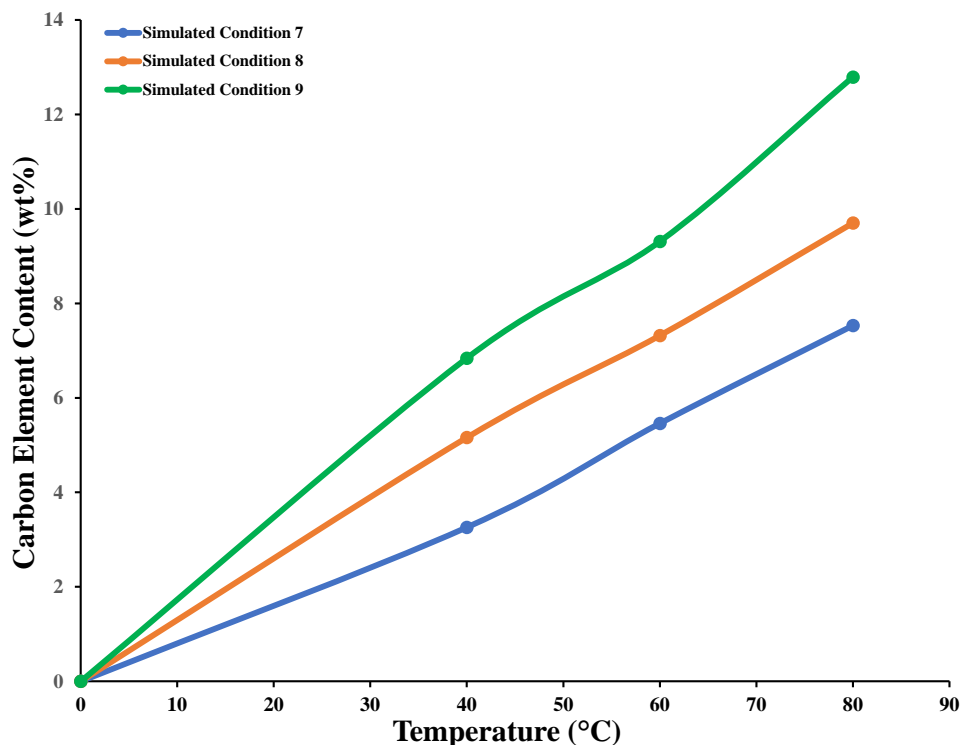

Figure 4.3: Graph of Carbon Element Content versus Temperature under Simulated Conditions 7, 8, and 9 at Relative Humidity of 80%.

The results of the samples have been reorganized based on the CO_2 conversion efficiency in descending order, as illustrated in Table 4.3. It is evident that the CO_2 conversion efficiency of sample 27, which is 12.79 %, is the highest among all 27 sets of samples. For comparison, the CO_2 conversion efficiency of sample 25 is 6.84 %, which undergone the mineralization process at the same concentration of CO_2 gas and humidity levels as sample 27 but at a temperature of 40 °C. It shows that as temperature increases from 40 °C to 80 °C, the carbonation efficiency has increased by approximately 87 %. The mean CO_2 conversion efficiencies of the mineralization conducted under various simulated

conditions at temperatures of 40 °C, 60 °C, and 80 °C are 3.00 %, 4.56 %, and 6.49 %, respectively.

Table 4.3:   Summary of CO$_2$ Conversion Efficiency for 27 Sets of Samples.

Sample No	CO$_2$ Conversion Efficiency (wt%)	Temperature (°C)	Concentration of CO$_2$ (%)	Humidity Levels (%)
27	12.79	80	30	80
24	9.7	80	20	80
26	9.31	60	30	80
18	8.31	80	30	60
21	7.53	80	10	80
23	7.32	60	20	80
25	6.84	40	30	80
15	6.44	80	20	60
17	6.11	60	30	60
20	5.46	60	10	80
22	5.16	40	20	80
14	4.71	60	20	60
12	4.61	80	10	60
16	4.22	40	30	60
9	3.55	80	30	40
19	3.26	40	10	80
13	3.19	40	20	60
6	3.02	80	20	40
11	2.64	60	10	60
8	2.56	60	30	40
3	2.48	80	10	40
5	1.89	60	20	40
10	1.55	40	10	60
7	1.46	40	30	40
4	0.99	40	20	40
2	0.97	60	10	40
1	0.36	40	10	40

4.3   Scanning Electron Microscopy (SEM)

The SEM test is conducted to identify the presence of crystal structures within the EAF slag samples after mineralization, indicating the formation of any carbonate minerals and determining which carbonate mineral is formed. The formation of carbonate minerals can be identified as the crystal structure of each carbonate mineral is different due to its unique atomic arrangement. In addition, many carbonate minerals like calcium carbonate and magnesium carbonate have polymorphs, meaning they can exist in different crystal structures while maintaining the same chemical composition. For example, polymorphs for calcium carbonate include calcite, vaterite, and aragonite.

According to the research (Ševčík, Petr Šašek and Viani, 2018), the morphology of synthetic $CaCO_3$ polymorphs varies based on synthesis conditions and the presence of additives or impurities. Each calcium carbonate polymorph may exhibit distinct crystal shapes due to differences in crystal structure. For instance, aragonite alone can display various morphologies such as hedgehog, cauliflower, spindle, flake, or hubbard squash-like structures. The SEM images with different magnifications of synthesised calcium carbonate polymorphs (a. calcite, b. aragonite, c. vaterite) are depicted in Figure 4.4.
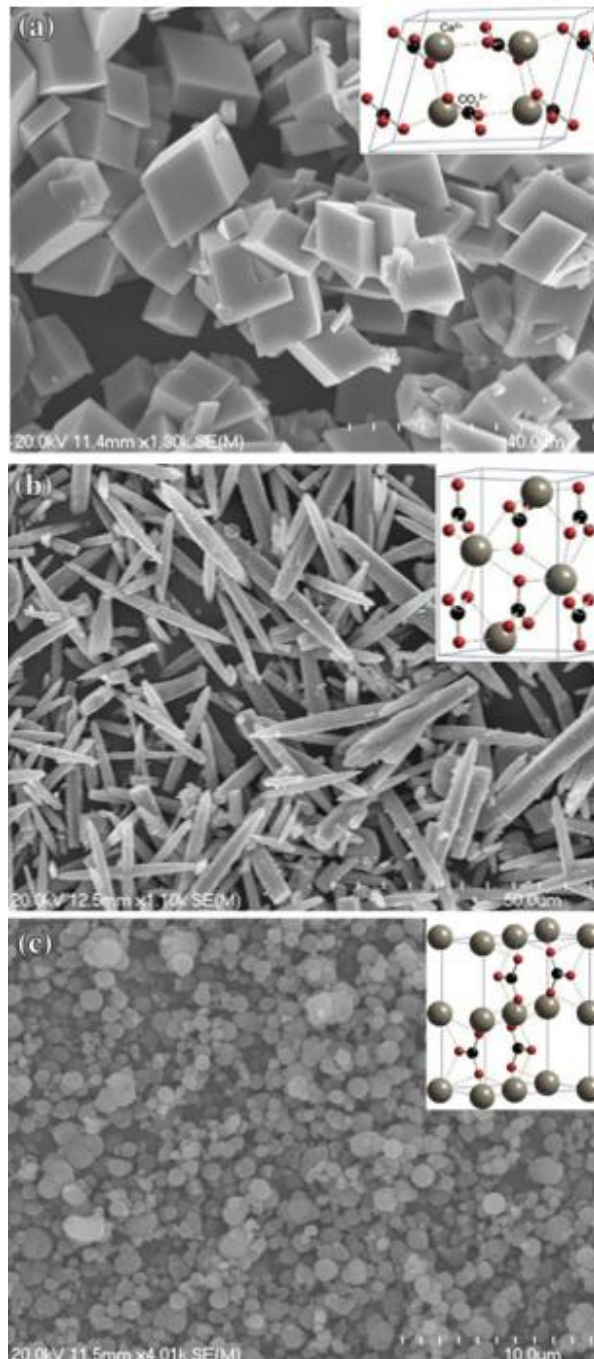
Figure 4.4: SEM Images of Synthesized Calcium Carbonate Polymorphs (a.
Calcite, b. Aragonite, c. Vaterite) (Seifan and Berenjian, 2018).

In addition, Figure 4.5 presents the typical morphology of the
synthesized calcium carbonates. The morphology depicted in the micrograph
indicates the presence of rod-like aragonite, rhombic-shaped calcite crystals,
and distributed round vaterite within the structure. However, the morphology of
the three calcium carbonate polymorphs in Figure 4.5 is different from Figure

4.4. This is because of the variations in preparation conditions may account for the observed irregularities in size and morphology (Abdou Elkoudy, et al., 2024).
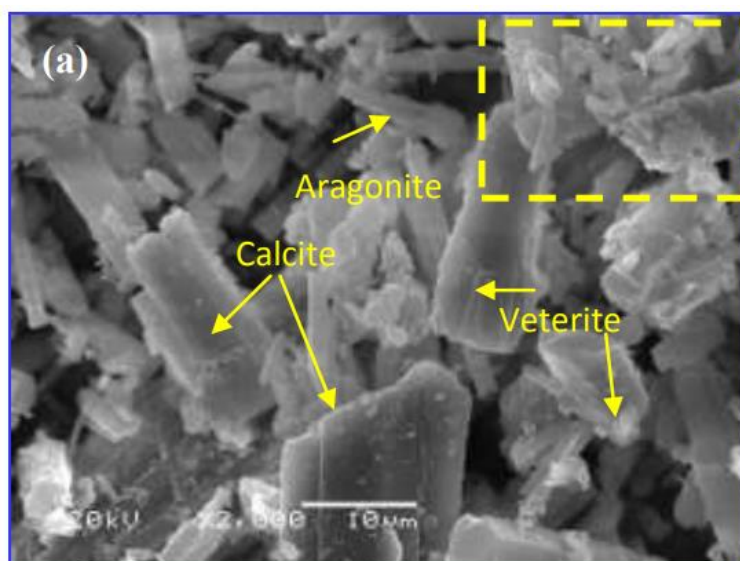
Figure 4.5: Typical Morphology of Synthesized Calcium Carbonates (Abdou Elkoudy, et al., 2024).

This research uses SEM to provide high-resolution images of the sample surfaces before and after mineralization. The SEM images, including uncarbonated EAF slag samples and 27 sets of EAF slag samples carbonated under different temperature parameters and simulated conditions, are taken with a magnification of 1,000 x, which enables capturing images of particle size of 50.0 µm. Figure 4.6 displays the SEM image of the EAF slag sample, with particle sizes ranging from 0.8 mm to 2.36 mm. It reveals the morphology and microstructure of the sample surfaces, clearly indicating the absence of crystal structures.

Figure 4.6: SEM Image of the EAF Slag Sample.

Figures 4.7a, 4.7b, 4.7c, and 4.7d demonstrate four SEM images illustrating distinct carbonated samples subjected to mineralization processes at 80°C. These samples were exposed to varying concentrations of CO_2 gas and humidity le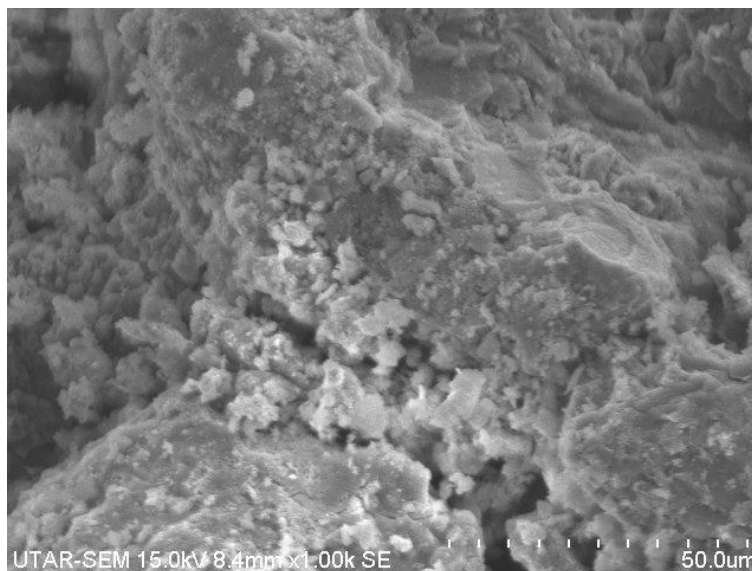vels. In addition, crystal structures were exclusively detected within the carbonated samples mineralized at 80 °C. Notably, no discernible crystal structures were observed in samples mineralized at 40 °C and 60 °C, despite detecting an increase in carbon element content using EDX analysis. The absence of crystal structures in the samples mineralized at 40 °C and 60 °C may be attributed to the lower temperatures impeding the formation of crystalline phases. Mineralization processes at these temperatures likely result in slower kinetics and insufficient energy for the development of well-defined crystal structures. The lower temperatures may also hinder the nucleation and growth of crystals, leading to the observed lack of crystallinity. This interpretation is supported by the increase in carbon element content detected in these samples using EDX analysis, indicating the presence of carbonaceous materials or amorphous phases formed under these conditions. Hence, it is imperative to utilize XRD analysis to ascertain the presence of calcium carbonate crystals in each carbonated sample.
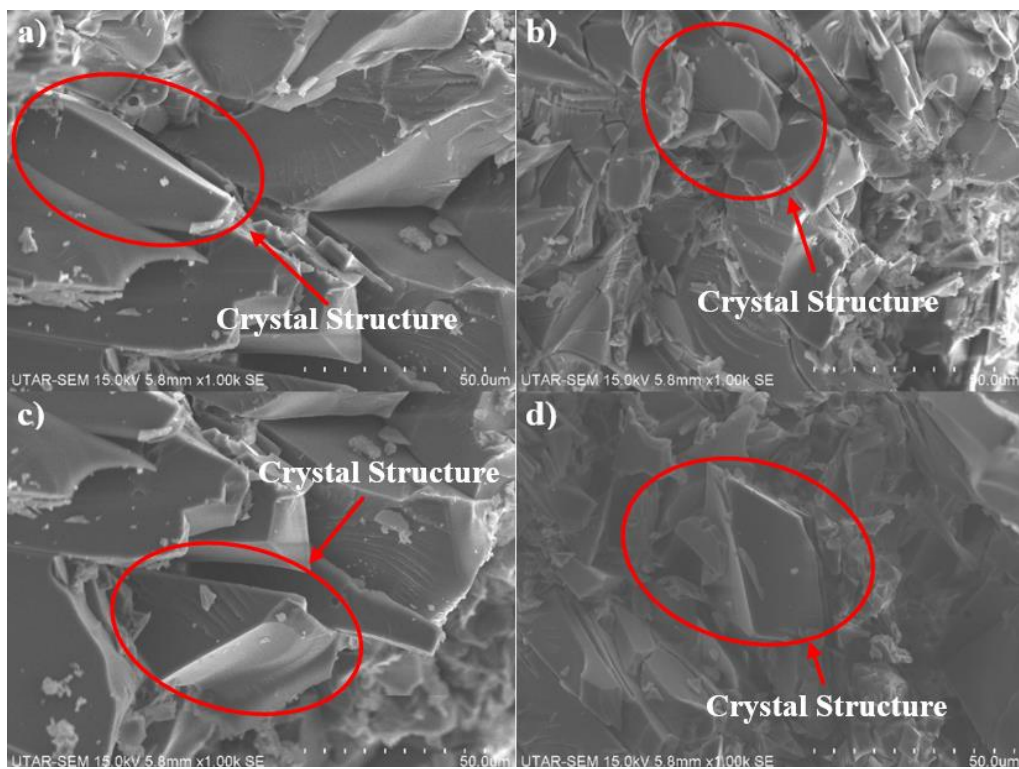
Figure 4.7: SEM Images of Distinct Carbonated Samples Subjected to
Mineralization Processes at 80 °C.

4.4   X-Ray Diffraction Analysis (XRD)

The XRD test was conducted on the EAF slag samples that had undergone mineralization processes under various temperature parameters and simulated conditions. In this study, XRD testing was performed to identify the crystalline phases present in EAF slags before and after mineralization, to provide quantitative information about the abundance or concentration of different mineral phases in the slag samples, and to identify any new mineral phases formed due to mineralization. The results obtained from the XRD test were further analysed using the software X'Pert Highscore Plus. Figures 4.8 to 4.10 display the XRD graphs of carbonated EAF slag samples that underwent mineralization at temperatures of 40 °C, 60 °C, and 80 °C, respectively. These processes were conducted under consistent conditions of 10 % concentration of CO_2 gas and 80 % relative humidity level.

        The XRD graphs in Figures 4.8 to 4.10 provide important information for the calcium carbonate crystals, including the peaks and their intensities. These peaks signify the positions of diffraction peaks, which correspond to the crystallographic planes within the material under analysis. Such peaks emerge when X-rays are diffracted by the crystal lattice of the sample at specific angles, known as Bragg angles, in accordance with Bragg's law. The intensity of the peaks in an XRD graph indicates the strength or magnitude of the diffracted X-rays at those angles. Higher intensity peaks typically denote higher concentrations or greater crystallinity of the corresponding crystalline phases within the sample. This intensity is measured as the number of X-ray photons detected by the XRD instrument at each angle of diffraction.
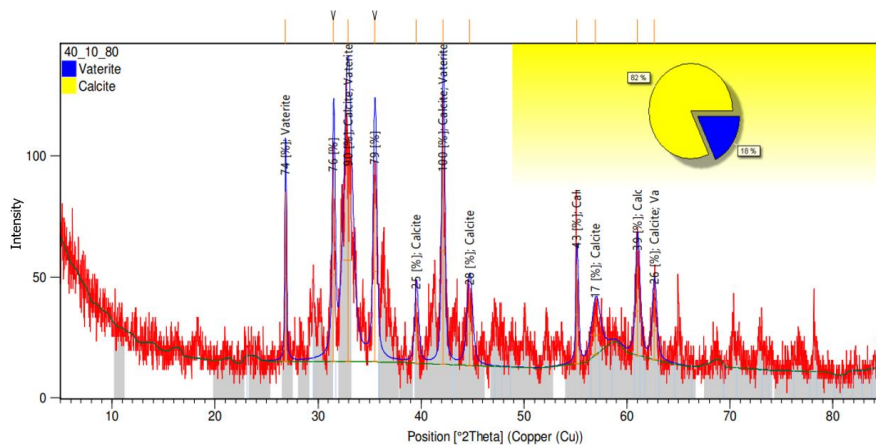
Figure 4.8: XRD Graph of Carbonated Sample that Underwent Mineralization
at a Temperature of 40 °C under Simulated Condition 7.
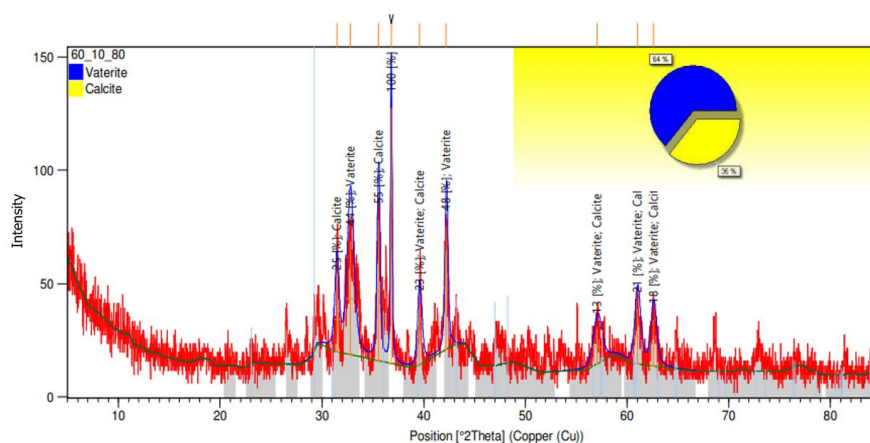
Figure 4.9: XRD Graph of Carbonated Sample that Underwent Mineralization
at a Temperature of 60 °C under Simulated Condition 7.
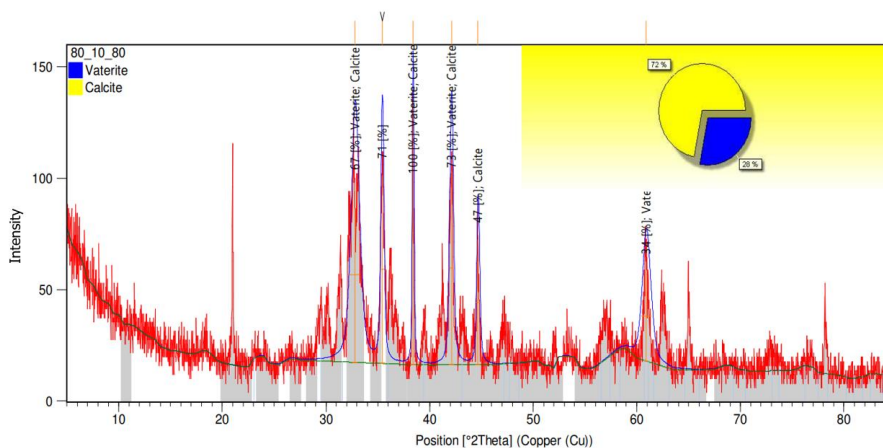
Figure 4.10: XRD Graph of Carbonated Sample that Underwent
Mineralization at a Temperature of 80 °C under Simulated
Condition 7.

Additionally, since the SEM test is unable to precisely identify the calcium carbonate polymorphs formed in the sample, the quantification chart feature in X'Pert Highscore Plus software has been utilized. This chart is employed to analyse and quantify the relative amounts or concentrations of different phases present in the sample based on X-ray diffraction (XRD) data. It provides information about the proportions of various crystalline phases identified in the sample, enabling researchers to determine the composition or mineralogy of the material under investigation. The quantification chart is generated by comparing the observed diffraction peaks in the XRD pattern with a database of known reference patterns for different crystalline phases. The software then calculates the relative intensities of these peaks and utilizes mathematical algorithms to estimate the percentage or weight percentage of each phase present in the sample. The relative amounts of the different crystalline phases, expressed as weight percentages, have been analysed, tabulated, and summarised for each sample, as shown in Table 4.4.

Table 4.4: Summary of the Relative Amounts of Different Crystalline Phases Present in the Samples.

Simulated Condition	Sample No	Temperature (°C)	Concentration of CO_2 gas (%)	Humidity (%)	Relative Amount of Different Crystalline Phases	
					Calcite (wt%)	Vaterite (wt%)
	1	40			21	79
1	2	60	10	40	28	72
	3	80			66	34
	4	40			21	79
2	5	60	20	40	18	82
	6	80			28	72
	7	40			27	73
3	8	60	30	40	63	37
	9	80			24	76
	10	40			34	66
4	11	60	10	60	20	80
	12	80			25	75
	13	40			55	45
5	14	60	20	60	52	48
	15	80			23	77
	16	40			39	61
6	17	60	30	60	8	92
	18	80			51	49

Table 4.4 (Continued)

	19	40			82	18
7	20	60	10	80	36	64
	21	80			72	28
	22	40			19	81
8	23	60	20	80	30	70
	24	80			42	58
	25	40			38	62
9	26	60	30	80	48	52
	27	80			25	75

Table 4.4 summarizes the relative amounts of different crystalline phases present in the samples, including calcite and vaterite, expressed as a percentage by weight. The results are further analysed by being plotted into two graphs, as shown in Figures 4.11 and 4.12, respectively. Figure 4.11 illustrates the graph of relative amount of calcite versus temperature. It shows that the relative amount of calcite in the carbonated samples across the simulated conditions generally increases from 0 °C to 40 °C. Subsequently, it exhibits a decrease as the temperature reaches 60 °C and then increases again from 60 °C to 80 °C. However, a deviation from this trend is observed in conditions 3, 5, 8, and 9. Specifically, at temperatures of 40 °C, 60 °C, and 80 °C, the pattern manifests as follows: in condition 3, an initial increase followed by another increase before declining; in condition 5, a similar initial increase followed by a subsequent decrease; in condition 8, a consistent increase throughout; and in condition 9, an initial rise followed by a decrease.
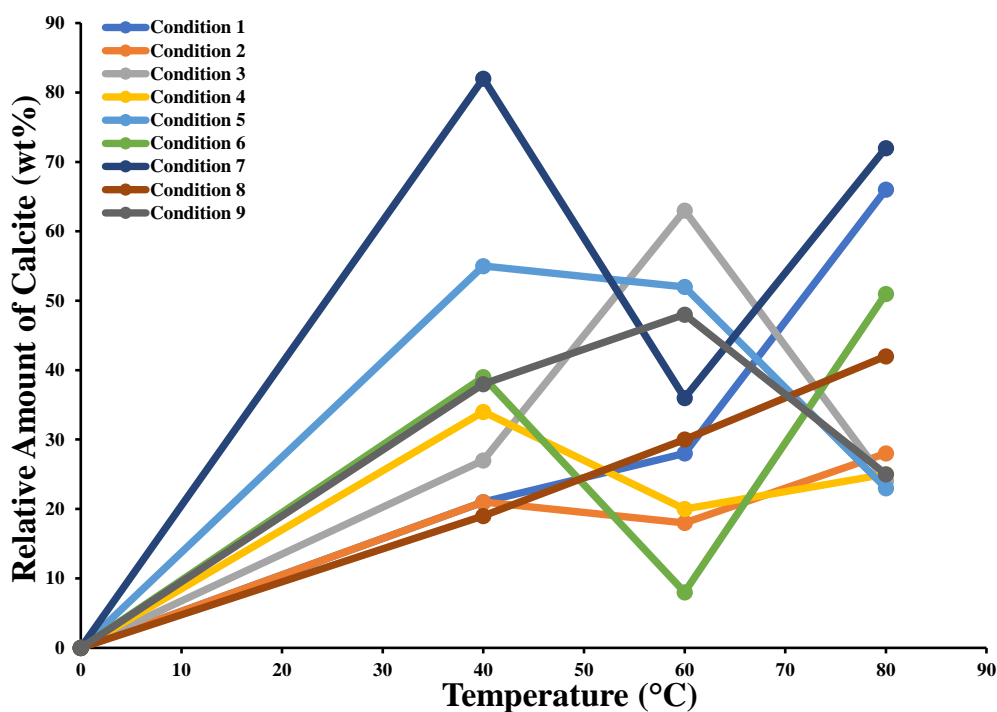

Figure 4.11: Graph of Relative Amount of Calcite versus Temperature.

Meanwhile, the graph in Figure 4.12 illustrates the relative amount of vaterite versus temperature. Considering that only two types of calcium carbonate polymorphs, calcite and vaterite, are present in the samples, the trend

in the relative amount of vaterite versus temperature for all samples across the nine simulated conditions is observed to be inversely proportional to the trend depicted in Figure 4.11, which displays the relative amount of calcite versus temperature.
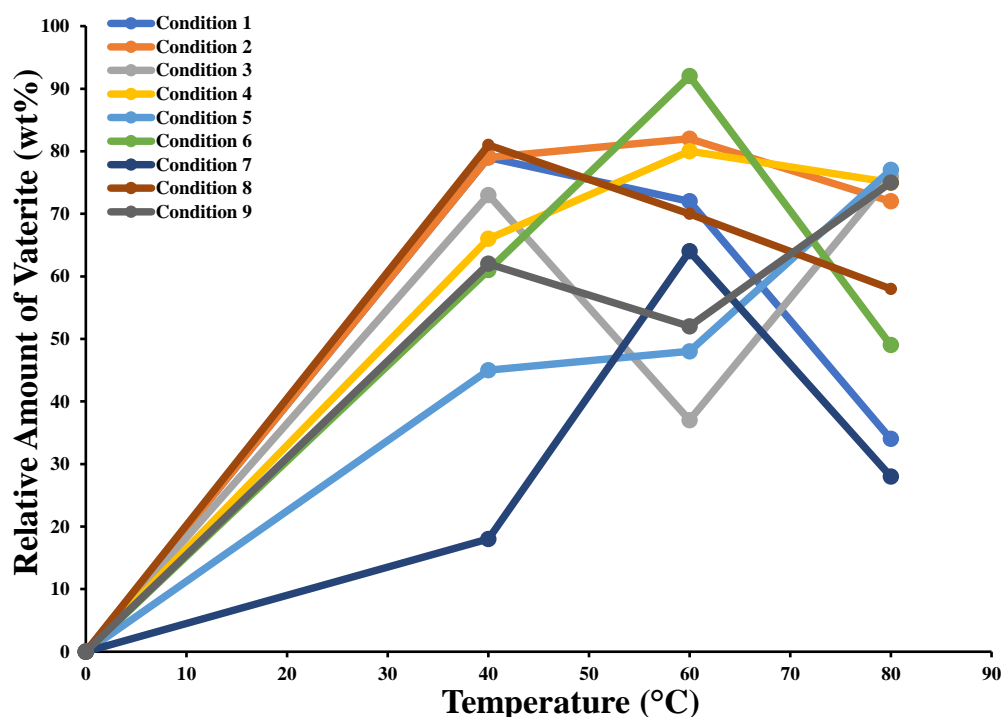
Figure 4.12: Graph of Relative Amount of Vaterite versus Temperature.

Additionally, it is observed that vaterite is more likely to be produced during the mineralization process of EAF slags. This is evidenced by the overall mean relative amount of vaterite among all three different temperatures, concentrations of CO_2 gas, and humidity levels, which has a mean weight percentage of approximately 63 %. At temperatures of 40 °C, 60 °C, and 80 °C, despite varying concentrations of CO_2 gas and humidity levels, the mean weight percentages of vaterite are 63 %, 66 %, and 60 %, respectively. According to the research (Chong, Chia and Zakaria, 2014), calcite typically forms at lower temperatures, around 20 °C to 30 °C. As the temperature increases, the abundance of calcite decreases, and the formation of vaterite becomes dominant. In addition, no aragonite is found within the samples due to its higher formation temperature compared to calcite and vaterite.

4.5 Thermogravimetric Analysis (TGA)

In this study, TGA tests were conducted to monitor changes in sample mass when subjected to controlled heating, to determine the carbonated samples' thermal stability. Specific conditions were established for the thermal analysis of the carbonated slag samples to ensure accurate measurement of their thermal properties. The analysis was performed under a nitrogen (N_2) atmosphere, with a continuous flow rate of 50 ml/min. A purge gas was also used at a flow rate of 20 ml/min to maintain a stable environment within the TGA instrument. The heating rate was set to 10 °C/min, allowing for a gradual increase in temperature over time. The temperature range extended from 25 °C to 900 °C, covering a broad spectrum to capture any changes in sample mass throughout the heating process. However, due to limited laboratory resources, only 9 out of the 27 carbonated samples underwent TGA tests.

Figures 4.13, to 4.15 demonstrate the TGA graphs of carbonated samples, namely samples 7, 8, and 9, respectively. Prior to the TGA test, these samples underwent a mineralization process at a 30 % concentration of CO_2, a 40 % humidity level, and under temperature parameters of 40 °C, 60 °C, and 80 °C, respectively. In Figure 4.13, it is shown that the sample mass experiences a small increase to roughly 100.4 % of the original mass as the temperature rises from 0 °C to approximately 50 °C. Then, it starts to decrease slowly to 100 % as the temperature rises until it reaches 300 °C. After that, it starts to decrease at a higher rate until around 800 °C and shows a small increase in mass to 99.4% until around 850 °C. Finally, it decreases gradually to 99.2 % of the original mass at a temperature of 900 °C.
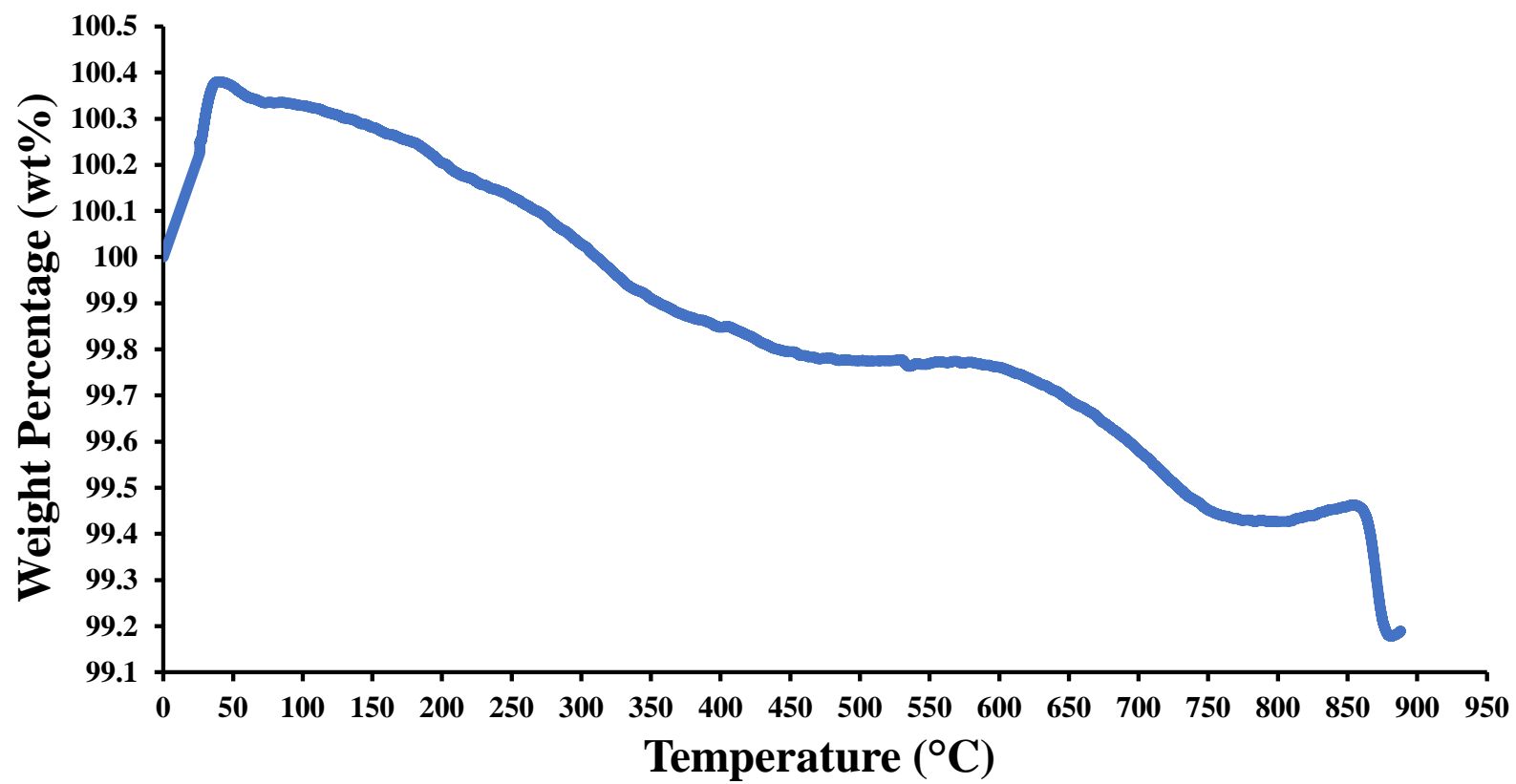
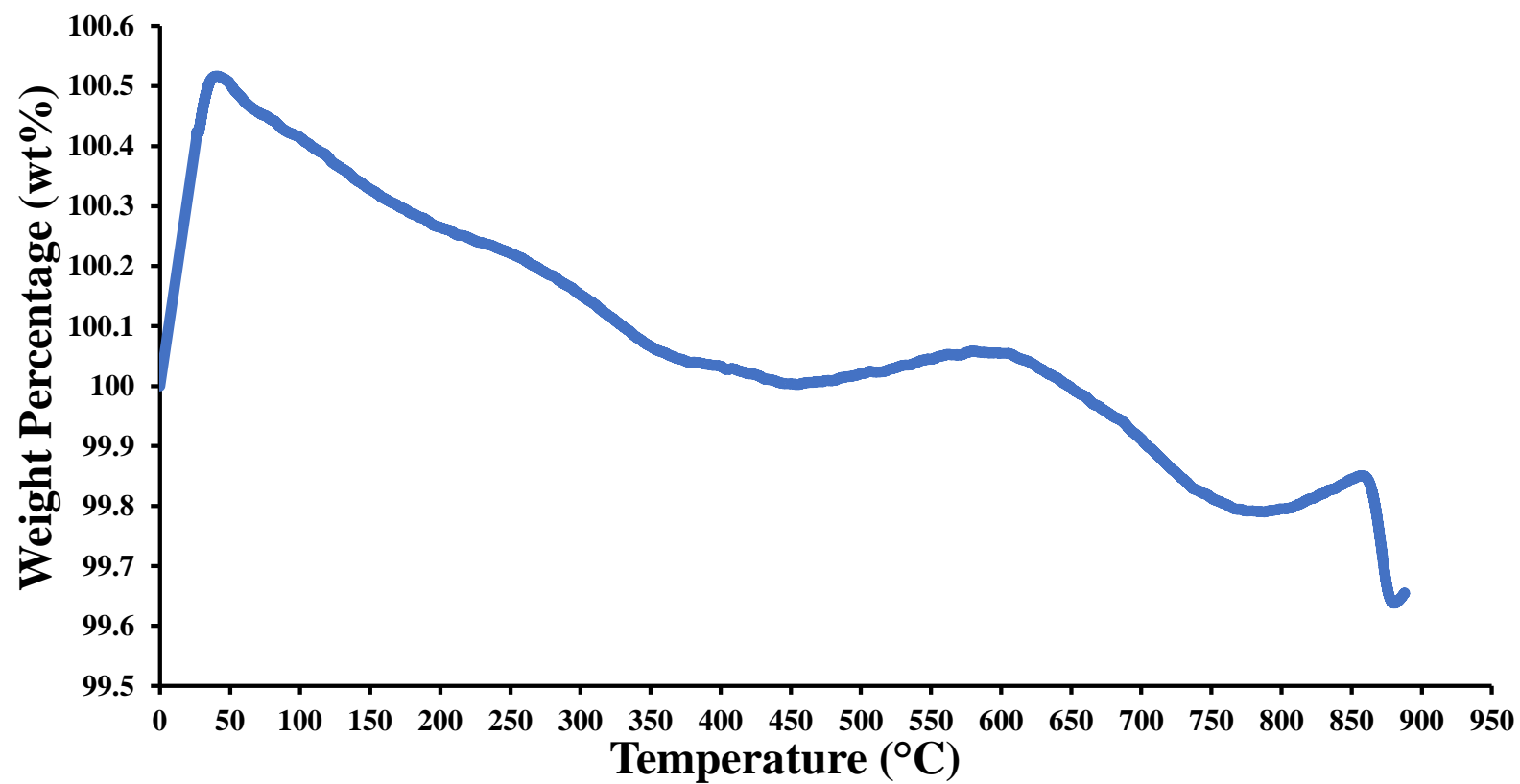Figure 4.13: TGA Graph of Carbonated Sample 7.
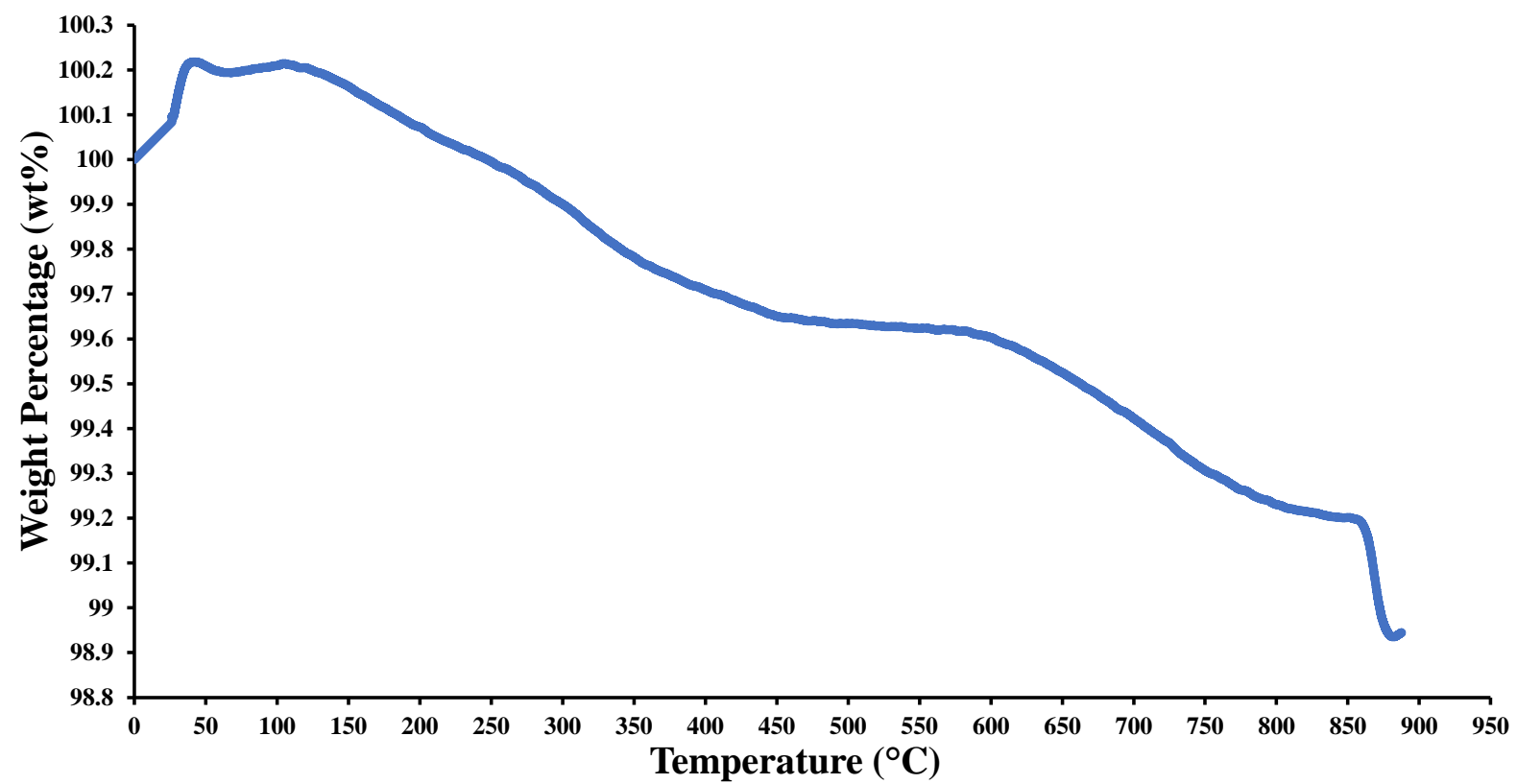
Figure 4.14: TGA Graph of Carbonated Sample 8.

Figure 4.15: TGA Graph of Carbonated Sample 9.

A similar pattern to that of the graph in Figure 4.13 is observed in Figures 4.14 and 4.15, which show a slight increase in sample mass to approximately 100.5 % and 100.2 %, respectively, as the temperature rises from 0 °C to 50 °C. Then, it starts to decrease slowly to 100 % as the temperatures rise until it reaches 450 °C and 300 °C, respectively. After that, the sample mass experiences a continuous decrease as temperatures continue to increase to approximately 800 °C. At 850 °C, the sample mass exhibits a slight increase to 99.9 % and 99.2 %, respectively. Finally, the mass decreases gradually to 99.6 % and 98.9 % at 900 °C.

Different patterns in TGA plots are observed across the other six samples that underwent mineralization processes at different temperatures, concentrations of CO_2, and humidity levels. The summary of the weight percentage of sample mass at different temperatures is further tabulated, as shown in Table 4.5 below. Samples 1, 2, and 3 underwent mineralization processes at 10 % CO_2 concentration and 40 % humidity levels at temperatures of 40 °C, 60 °C, and 80 °C, respectively. Samples 4, 5, and 6 underwent mineralization processes at 20 % CO_2 concentration and 60 % humidity levels at temperatures of 40 °C, 60 °C, and 80 °C, respectively. Similarly, samples 7, 8, and 9 underwent mineralization processes at 30 % CO_2 concentration and 80 % humidity levels at temperatures of 40 °C, 60 °C, and 80 °C, respectively.

Although several instances of mass reduction in the samples at different temperature ranges are observed, mass loss may occur due to the dehydration, oxidation or combustion of other compounds, such as organic compounds and other impurities in the samples. Based on the findings of Li, et al. (2017), calcium carbonate exhibits weight loss exclusively within the temperature range of 600 °C to 850 °C. In a different investigation, Gao, et al. (2013) observed that carbonated samples containing different amounts of $CaCO_3$ display strong thermal stability, with no notable mass loss detected up to 360 °C. Additionally, the summarized results reveal that the greatest mass reduction, amounting to 4.60 %, occurs in sample 4, while the mean mass loss across all samples is 1.91 %. A mass reduction of 4.60 % may not necessarily indicate thermal instability for carbonated steel slags. Whether this level of mass reduction is considered thermally stable depends on various factors, such as the composition of the slag, the specific application, and the desired properties.

Table 4.5:   Summary of Weight Percentage of Sample Mass at Different
Temperatures.

Sample	Temperature (°C)	Weight Percentage of Sample Mass (wt%)
1	50	99.60
	300	100.0
	800	97.4
	900	97.3
2	50	100.2
	300	100.0
	800	99.9
	900	99.9
3	50	98.7
	300	98.3
	800	96.4
	900	96.2
4	50	98.8
	300	98.2
	800	95.6
	900	95.4
5	50	100.2
	300	100.0
	800	99.9
	900	99.7
6	50	100.3
	300	99.8
	850	97.3
	900	97.2
7	50	100.4
	300	100.0
	850	99.4
	900	99.2
8	50	100.5
	300	100.2
	850	99.9
	900	99.6
9	50	100.2
	300	100.0
	850	99.2
	900	98.9

4.6   Summary

This chapter presents comprehensive results obtained from various laboratory tests, including Energy-Dispersive X-ray Spectroscopy (EDX), Scanning Electron Microscopy (SEM), X-ray Diffraction Analysis (XRD), and Thermogravimetric Analysis (TGA).

The SEM test revealed visible crystal structures in the mineralized EAF slag samples only when subjected to mineralization at 80 °C. The XRD analysis confirmed the presence of calcium carbonate in all mineralized samples, despite the varying temperatures and simulated conditions. Among the identified polymorphs, 63 % were vaterite, while 37 % were calcite.

Results from the EDX test indicated a positive correlation between temperature and CO_2 conversion efficiency, showing an increasing trend as temperatures rose. The maximum CO_2 conversion efficiency of 12.79 % was achieved under conditions of 80 °C, 30 % CO_2 concentration, and 80 % relative humidity.

The TGA test showed a mean weight reduction of only 2 % in the sample formed under optimized conditions when heated up to approximately 900 °C. Additionally, the greatest mass reduction of 4.60 % occurred in samples mineralized at 40 °C, 20 % CO_2 concentration, and 60 % humidity. The average mass loss across all tested samples was 1.91 %.

CHAPTER 5

CONCLUSIONS AND RECOMMENDATIONS

5.1 Conclusions

In summary, this study investigates the CO_2 conversion efficiency of Electric Arc Furnace (EAF) slag mineralization across varying temperature parameters (40 °C, 60 °C, and 80 °C) and simulated conditions, including different CO_2 gas concentrations (10 %, 20 %, and 30 %) and relative humidity levels (40 %, 60 %, and 80 %). The study aims to determine the optimal temperature influencing the mineralization process, aiming for maximized CO_2 conversion efficiency and formation of thermally stable carbonate minerals.

The first objective of this study is to investigate the effect of different temperatures on the mineralization process. Results from Energy-Dispersive X-ray spectroscopy (EDX) testing indicate a positive correlation between temperature parameters and the CO_2 conversion efficiency of mineralization, showing an increasing trend as temperatures rise. Scanning Electron Microscopy (SEM) testing reveals the presence of visible crystal structures in the EAF slag samples only when subjected to mineralization at 80°C. X-ray diffraction Analysis (XRD) reveals the presence of calcium carbonate in all samples, despite mineralization being conducted under varying temperatures and simulated conditions. Among these polymorphs identified, 63 % are vaterite, while the remaining 37 % are calcite.

The second objective of this study is to identify the maximized CO_2 conversion efficiency of the mineralization process under varying conditions. The study identifies the maximum CO_2 conversion efficiency as 12.79 %, achieved under experimental parameters of 80 °C temperature, 30 % CO_2 gas concentration, and 80 % relative humidity levels.

The third objective of this study is to determine the thermal stability of the carbonate minerals that formed under the optimized temperature and CO_2 conversion conditions. Thermogravimetric Analysis (TGA) indicates only a 2 % weight reduction in the sample formed under optimized temperature and CO_2 conversion efficiency when subjected to heating up to approximately 900 °C.

5.2   Recommendations for Future Work

This study focuses solely on maximizing CO_2 conversion efficiency and ensuring the formation of thermally stable carbonate minerals by optimizing the temperature parameters in the mineralization process of electric arc furnace (EAF) slag. However, the effects of different temperatures on the mineralization process are limited to the range of 40 °C to 80 °C, with temperature intervals of 20 °C. Additionally, the study only utilizes one type of steel slag in the mineralization process, which may limit the ability to validate the optimal temperature for CO_2 conversion efficiency. Hence, it is imperative to conduct an in-depth study of the effects of a wider range of temperature parameters on the mineralization of various slags. Here are some recommendations for future work:

(i)   Conduct experiments using a wider range of temperature parameters. Explore lower and higher temperatures to assess their impact on CO_2 conversion efficiency and mineralization kinetics. This comprehensive approach can provide a more thorough understanding of the temperature dependence of the process and help identify potential temperature thresholds for optimizing CO_2 conversion.

(ii)   Within each temperature range, refine the intervals to smaller increments to capture subtle variations in CO_2 conversion efficiency and mineralization behaviour. This finer resolution will enable more precise identification of optimal temperature thresholds and facilitate a detailed analysis of temperature effects on the process.

(iii)   Conducting a thorough exploration of various types of steel slags is essential to validate the optimal temperature for CO_2 conversion efficiency and mineralization kinetics. This approach ensures comprehensive coverage of potential variations in CO_2 mineralization behaviour by encompassing a wide array of slag compositions and characteristics.

REFERENCES

Abanades, J.C., Allam, R., Lackner, K.S., Meunier, F., Rubin, E., Sanchez, J.C., Yogo, K., Zevenhoven, R. and Mazzotti, M., 2005. *Mineral Carbonation and Industrial Uses of Carbon Dioxide.* [online] IPCC WG-III: Cambridge University Press, pp.321–335. Available at: https://www.ipcc.ch/site/assets/uploads/2018/03/srccs_chapter7-1.pdf [Accessed 15 August 2023].

Abdou, E., Essa, M., Ahmed, E. and Suliman, M., 2024. Feasible Calcium Carbonate Polymorphs Synthesis from Natural Corallines and Their Potential Gelling Role in Hydraulic Fracturing Application. *Assiut University Journal of Multidisciplinary Scientific Research*, [e-journal] 53(1), pp.57–73. https://doi.org/10.21608/aunj.2023.226733.1060.

Altantzis, I., 2023. Enhancing Mineral Carbonation of Olivine with CO2. *An Experimental Study on Particle Size and Assessment of the CO2 Dissolution Rate through the Overall Mass Transfer Coefficient (kLa)*, [online] 1(1). Available at: https://kth.diva-portal.org/smash/record.jsf?pid=diva2%3A1769208&dswid=1657 [Accessed 16 August 2023].

Azdarpour, A., Asadullah, M., Junin, R., Manan, M., Hamidi, H. and Daud, A.R.M., 2014. Carbon Dioxide Mineral Carbonation through pH-swing Process: A Review. *Energy Procedia*, [e-journal] 61, pp.2783–2786. https://doi.org/10.1016/j.egypro.2014.12.311.

Azdarpour, A., Asadullah, M., Mohammadian, E., Hamidi, H., Junin, R. and Karaei, M.A., 2015. A Review on Carbon Dioxide Mineral Carbonation through pH-swing Process. *Chemical Engineering Journal*, [e-journal] 279, pp.615–630. https://doi.org/10.1016/j.cej.2015.05.064.

Baras, A., Li, J., Wen, N., Hussain, Z. and Hitch, M., 2023. Evaluation of Potential Factors Affecting Steel Slag Carbonation. *Processes 2023*, [e-journal] 11(9), pp.2590–2590. https://doi.org/10.3390/pr11092590.

Bunaciu, A., Udriştioiu, E. and Aboul-Enein, H.Y., 2015. X-Ray Diffraction: Instrumentation and Applications. *Critical Reviews in Analytical Chemistry*, [e-journal] 45(4), pp.289–299. https://doi.org/10.1080/10408347.2014.949616.

Carteret, C., Dandeu, A., Humbert, B., Moussaoui, S., Muhr, H. and Plasari, E., 2008. Polymorphism Studied by Lattice Phonon Raman Spectroscopy and Statistical Mixture Analysis Method. Application to Calcium Carbonate Polymorphs during Batch Crystallization. *Crystal Growth & Design*, [e-journal] 9(2), pp.807–812. https://doi.org/10.1021/cg800368u.

Chang, R., Choi, D., Kim, M.H. and Park, Y., 2016. Tuning Crystal Polymorphisms and Structural Investigation of Precipitated Calcium Carbonates for CO2 Mineralization. *ACS Sustainable Chemistry & Engineering*, [e-journal] 5(2), pp.1659–1667. https://doi.org/10.1021/acssuschemeng.6b02411.

Chang, R., Kim, S., Lee, S., Choi, S., Kim, M. and Park, Y., 2017. Calcium Carbonate Precipitation for CO2 Storage and Utilization: A Review of the Carbonate Crystallization and Polymorphism. *Frontiers in Energy Research*, [e-journal] 5(17), pp.1–9. https://doi.org/10.3389/fenrg.2017.00017.

Chen, Z., Cang, Z., Yang, F., Zhang, J. and Zhang, L., 2021. Carbonation of steelmaking slag presents an opportunity for carbon neutral: A review. Journal of CO2 Utilization, [e-journal] 54, pp.101738. https://doi.org/10.1016/j.jcou.2021.101738.

Chiang, P.C., Chen, C.D., Chang, E.E., Pan, S.Y., Chen, Y.H. and Lin, H.Y., 2013. Systematic Approach to Determination of Maximum Achievable Capture Capacity via Leaching and Carbonation Processes for Alkaline Steelmaking Wastes in a Rotating Packed Bed. *Environmental Science & Technology*, [e-journal] 47(23), pp.13677–13685. https://doi.org/10.1021/es403323x.

Chong, K.L., Chia, C.H. and Zakaria, S., 2014. Polymorphs Calcium Carbonate on Temperature Reaction. *AIP Conference Proceedings*, [e-journal] 1614(1), pp.52–56. https://doi.org/10.1063/1.4895169.

Gao, W., Ma, X., Liu, Y., Wang, Z. and Zhu, Y., 2013. Effect of Calcium Carbonate on PET Physical Properties and Thermal Stability. *Powder Technology*, [e-journal] 244, pp.45–51. https://doi.org/10.1016/j.powtec.2013.04.008.

Ghacham, A.B., Pasquier, L.C., Cecchi, E., Blais, J.F. and Mercier, G., 2016. CO2 Sequestration by Mineral Carbonation of Steel Slags under Ambient temperature: Parameters influence, and Optimization. *Environmental Science and Pollution Research*, [e-journal] 23(17), pp.17635–17646. https://doi.org/10.1007/s11356-016-6926-4.

Hodoroaba, V.D., 2020. Energy-dispersive X-ray Spectroscopy (EDS). *Micro and Nano Technologies*, [e-journal] 4(4), pp.397–417. https://doi.org/10.1016/b978-0-12-814182-3.00021-3.

Huijgen, W.J.J. and Comans, R.N.J., 2005a. *Carbon Dioxide Storage by Mineral Carbonation.* [online] *IEA Greenhouse Gas R&D Programme.* Available at: https://ieaghg.org/docs/General_Docs/Reports/2005-11%20CO2%20mineralisation.pdf [Accessed 15 August 2023].

Huijgen, W.J.J. and Comans, R.N.J., 2005b. Mineral CO2 Sequestration by Steel Slag Carbonation. *Environmental Science & Technology*, [e-journal] 39(24), pp.9676–9682. https://doi.org/10.1021/es050795f.

Jo, H., Park, S.H., Jang, Y.N., Chae, S.C., Lee, P.K., and Jo, H.Y., 2014. Metal Extraction and Indirect Mineral Carbonation of Waste Cement Material Using Ammonium Salt Solutions. *Chemical Engineering Journal*, [e-journal] 254, pp.313–323. https://doi.org/10.1016/j.cej.2014.05.129.

Karunadasa, K.S.P., Manoratne, C.H., Pitawala, H.M.T.G.A. and Rajapakse, R.M.G., 2019. Thermal Decomposition of Calcium Carbonate (calcite polymorph) as Examined by in-situ high-temperature X-ray Powder Diffraction. *Journal of Physics and Chemistry of Solids*, [e-journal] 134, pp.21–28. https://doi.org/10.1016/j.jpcs.2019.05.023.

Ko, M.S., Chen, Y.L. and Jiang, J.H., 2015. Accelerated Carbonation of Basic Oxygen Furnace Slag and the Effects on Its Mechanical Properties. *Construction and Building Materials*, [e-journal] 98, pp.286–293. https://doi.org/10.1016/j.conbuildmat.2015.08.051.

Li, X., Lv, Y., Ma, B., Wang, W. and Jian, S., 2017. Decomposition Kinetic Characteristics of Calcium Carbonate Containing Organic Acids by TGA. *Arabian Journal of Chemistry*, [e-journal] 10(2), pp.2534–2538. https://doi.org/10.1016/j.arabjc.2013.09.026.

Liendo, F., Arduino, M., Deorsola, F.A. and Bensaid, S., 2022. Factors controlling and influencing polymorphism, morphology and size of calcium carbonate synthesized through the carbonation route: A review. *Powder Technology*, [e-journal] 398, pp.117050. https://doi.org/10.1016/j.powtec.2021.117050.

Liu, Q., Liu, J. and Qi, L., 2016. Effects of Temperature and Carbonation Curing on the Mechanical Properties of Steel slag-cement Binding Materials. *Construction and Building Materials*, [e-journal] 124, pp.999–1006. https://doi.org/10.1016/j.conbuildmat.2016.08.131.

Loganathan, S., Valapa, R.B., Mishra, R.K., Pugazhenthi, G. and Thomas, S., 2017. Thermogravimetric Analysis for Characterization of Nanomaterials. *Thermal and Rheological Measurement Techniques for Nanomaterials Characterization*, [e-journal] 4(1), pp.67–108. https://doi.org/10.1016/b978-0-323-46139-9.00004-9.

Mohammed, A. and Abdullah, A., 2018. Scanning Electron Microscopy (Sem): A Review. *Proceedings of 2018 International Conference on Hydraulics and Pneumatics*, [online] 7(9). Available at: http://hervex.ro/hervex-2018-proc-toc/ [Accessed 30 March 2024].

Neeraj and Yadav, S., 2020. Carbon Storage by Mineral Carbonation and Industrial Applications of CO2. *Materials Science for Energy Technologies*, [e-journal] 3, pp.494–500. https://doi.org/10.1016/j.mset.2020.03.005.

Nicol, A.W., 2012. *Physicochemical Methods of Mineral Analysis*. [e-book] Springer eBooks: Springer Nature. Available through: https://link.springer.com/book/10.1007/978-1-4684-2046-3 [Accessed 27 March 2024].

Nielsen, P., Boone, M.A., Horckmans, L., Snellings, R. and Quaghebeur, M., 2020. Accelerated Carbonation of Steel Slag Monoliths at Low CO2 Pressure – Microstructure and Strength Development. *Journal of CO2 Utilization*, [e-journal] 36, pp.124–134. https://doi.org/10.1016/j.jcou.2019.10.022.

Pan, S.Y., Chen, Y.H., Fan, L.S., Kim, H., Gao, X., Ling, T.C., Chiang, P.C., Pei, S.L. and Gu, G., 2020. CO2 Mineralization and Utilization by Alkaline Solid Wastes for Potential Carbon Reduction. *Nature Sustainability*, [e-journal] 3(5), pp.399–405. https://doi.org/10.1038/s41893-020-0486-9.

Pan, S.Y., Ling, T.C., Ah-Hyung Alissa Park and Chiang, P.C., 2018. An Overview: Reaction Mechanisms and Modelling of CO2 Utilization via Mineralization. *Aerosol and Air Quality Research*, [e-journal] 18(4), pp.829–848. https://doi.org/10.4209/aaqr.2018.03.0093.

Polettini, A., Pomi, R. and Stramazzo, A., 2016. Carbon sequestration through accelerated carbonation of BOF slag: Influence of particle size characteristics. *Chemical Engineering Journal*, 298, pp.26–35. https://doi.org/10.1016/j.cej.2016.04.015.

Prigiobbe, V., Polettini, A. and Baciocchi, R., 2009. Gas-Solid Carbonation Kinetics of Air Pollution Control Residues for CO2 Storage. *Chemical Engineering Journal*, [e-journal] 148(2-3), pp.270–278. https://doi.org/10.1016/j.cej.2008.08.031.

Quaghebeur, M., Nielsen, P., Horckmans, L. and Van Mechelen, D., 2015. Accelerated Carbonation of Steel Slag Compacts: Development of High-Strength Construction Materials. *Frontiers in Energy Research*, [e-journal] 3(1), pp.3–52. https://doi.org/10.3389/fenrg.2015.00052.

Rađenović, A., Malina, J. and Sofilić, T., 2013. Characterization of Ladle Furnace Slag from Carbon Steel Production as a Potential Adsorbent. *Advances in Materials Science and Engineering*, [e-journal] 2013, pp.1–6. https://doi.org/10.1155/2013/198240.

Radha, A.V. and Navrotsky, A., 2013. Thermodynamics of Carbonates. *Reviews in Mineralogy and Geochemistry*, [e-journal] 77(1), pp.1–14. https://doi.org/10.2138/rmg.2013.77.1.

Rahmanihanzaki, M. and Hemmati, A., 2022. A Review of Mineral Carbonation by Alkaline Solidwaste. *International Journal of Greenhouse Gas Control*, [e-journal] 121, pp.103798. https://doi.org/10.1016/j.ijggc.2022.103798.

Ramli, N.A.A., Kusin, F.M. and Molahid, V.L.M., 2021. Influencing Factors of the Mineral Carbonation Process of Iron Ore Mining Waste in Sequestering Atmospheric Carbon Dioxide. *Sustainability*, [e-journal] 13(4), pp.1866. https://doi.org/10.3390/su13041866.

Sanna, A., Uibu, M., Caramanna, G., Kuusik, R. and M. Maroto-Valer, M., 2014. A Review of Mineral Carbonation Technologies to Sequester CO2. *Chemical Society Reviews*, [e-journal] 43(23), pp.8049–8080. https://doi.org/10.1039/C4CS00035H.

Seifan, M. and Berenjian, A., 2018. Application of Microbially Induced Calcium Carbonate Precipitation in Designing Bio self-healing Concrete. *World Journal of Microbiology and Biotechnology*, [e-journal] 34(168), pp.1–15. https://doi.org/10.1007/s11274-018-2552-2.

Ševčík, R., Petr Šašek and Viani, A., 2018. Physical and Nanomechanical Properties of the Synthetic Anhydrous Crystalline CaCO3 polymorphs: vaterite, Aragonite and Calcite. *Journal of Materials Science*, [e-journal] 53(6), pp.4022–4033. https://doi.org/10.1007/s10853-017-1884-x.

Shen, Y., 2023. Molten Salt-Mediated Carbon Capture and Conversion. *Fuel*, [e-journal] 339, pp.127473. https://doi.org/10.1016/j.fuel.2023.127473.

Shindo, D. and Oikawa, T., 2002. Energy Dispersive X-ray Spectroscopy. *Analytical Electron Microscopy for Materials Science*, [e-journal] 4(1), pp.81–102. https://doi.org/10.1007/978-4-431-66988-3_4.

Song, Q., Guo, M.Z., Wang, L. and Ling, T.C., 2021. Use of steel slag as sustainable construction materials: A review of accelerated carbonation treatment. *Resources, Conservation and Recycling*, [e-journal] 173, pp.105740. https://doi.org/10.1016/j.resconrec.2021.105740.

Teir, S., Eloneva, S., Fogelholm, C.J. and Zevenhoven, R., 2006. Stability of Calcium Carbonate and Magnesium Carbonate in Rainwater and Nitric Acid Solutions. *Energy Conversion and Management*, [e-journal] 47(18-19), pp.3059–3068. https://www.sciencedirect.com/science/article/pii/S0196890406000987.

Wang, L., Sarkar, B., Sonne, C., Ok, Y.S. and Tsang, D.C.W., 2020. Soil and Geologic Formations as Antidotes for CO2 Sequestration? *Soil Use and Management*, [e-journal] 36(3), pp.355–357. https://doi.org/10.1111/sum.12589.

Wang, X. and Maroto-Valer, M.M., 2011. Integration of CO2 Capture and Mineral Carbonation by Using Recyclable Ammonium Salts. *ChemSusChem*, [e-journal] 4(9), pp.1291–1300. https://doi.org/10.1002/cssc.201000441.

Wei, X., Wen, N., Zhang, S., Wang, X., Li, J. and Du, H., 2022. Influence of the Key Factors on the Performance of Steel Slag-Desulphurisation Gypsum-Based Hydration-Carbonation Materials. *Journal of Building Engineering*, [e-journal] 45, pp.103591–103591. https://doi.org/10.1016/j.jobe.2021.103591.

Wells, R.C., 1934. The Thermal Decomposition of Some Carbonate Minerals. *Transactions, American Geophysical Union*, [e-journal] 15(1), pp.237–240. https://doi.org/10.1029/tr015i001p00237.

Whittig, L.D. and Allardice, W.R., 2018. X-Ray Diffraction Techniques. *SSSA Book Series*, [e-journal] 5(1), pp.331–362. https://doi.org/10.2136/sssabookser5.1.2ed.c12.

Wilson, S.A., Barker, S.L.L., Dipple, G.M. and Atudorei, V., 2010. Isotopic Disequilibrium during Uptake of Atmospheric CO_2 into Mine Process Waters: Implications for CO_2 Sequestration. *Environmental Science & Technology*, [e-journal] 44(24), pp.9522–9529. https://doi.org/10.1021/es1021125.

Xiao, S., Chen, X., Qi, L. and Liu, Y., 2019. A Review of Mineral Carbonation from Industrial Waste. *IOP Conference Series: Earth and Environmental Science*, [e-journal] 401(1), pp.012008–012008. https://doi.org/10.1088/1755-1315/401/1/012008.

Yadav, S. and Mehra, A., 2021. A Review on Ex Situ Mineral Carbonation. *Environmental Science and Pollution Research*, [e-journal] 28(10), pp.12202–12231. https://doi.org/10.1007/s11356-020-12049-4.

Yong, X., Tse, J.S. and Chen, J., 2018. Mechanism of Chemical Reactions between SiO2 and CO2 under Mantle Conditions. *ACS Earth and Space Chemistry*, [e-journal] 2(6), pp.548–555. https://doi.org/10.1021/acsearthspacechem.7b00144.

Yu, J. and Wang, K., 2011. Study on Characteristics of Steel Slag for CO_2Capture. *Energy & Fuels*, [e-journal] 25(11), pp.5483–5492. https://doi.org/10.1021/ef2004255.

Zhang, N., Chai, Y.E., Santos, R.M. and Šiller, L., 2020. Advances in Process Development of Aqueous CO2 Mineralisation Towards Scalability. *Journal of Environmental Chemical Engineering*, [e-journal] 8(6), pp.104453. https://doi.org/10.1016/j.jece.2020.104453.

Zhao, H., Park, Y., Lee, D.H. and Park, A.H.A., 2013. Tuning the Dissolution Kinetics of Wollastonite via Chelating Agents for CO2 Sequestration with Integrated Synthesis of Precipitated Calcium Carbonates. *Physical Chemistry Chemical Physics*, [e-journal] 15(36), pp.15185. https://doi.org/10.1039/c3cp52459k.